

PromptSplit: Revealing Prompt-Level Disagreement in Generative Models

Mehdi Lotfian¹, Mohammad Jalali¹, Farzan Farnia¹

¹Department of Computer Science and Engineering, The Chinese University of Hong Kong
 lotfian25@cse.cuhk.edu.hk, mjalali24@cse.cuhk.edu.hk, farnia@cse.cuhk.edu.hk

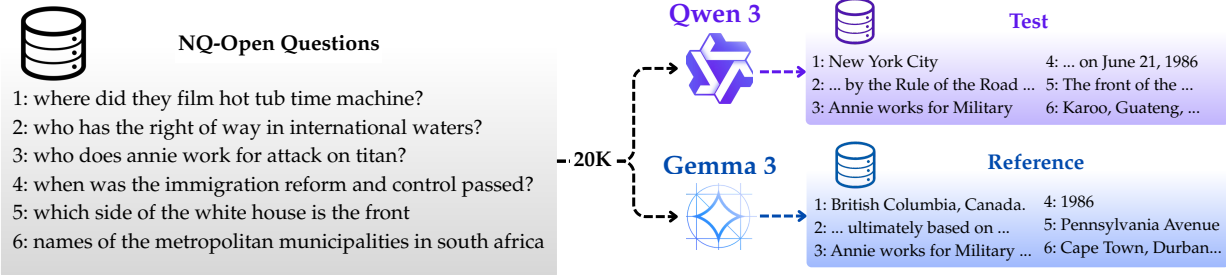
Abstract

Prompt-guided generative AI models have rapidly expanded across vision and language domains, producing realistic and diverse outputs from textual inputs. The growing variety of such models, trained with different data and architectures, calls for principled methods to identify which types of prompts lead to distinct model behaviors. In this work, we propose PromptSplit, a kernel-based framework for detecting and analyzing prompt-dependent disagreement between generative models. For each compared model pair, PromptSplit constructs a joint prompt–output representation by forming tensor-product embeddings of the prompt and image (or text) features, and then computes the corresponding kernel covariance matrix. We utilize the eigenspace of the weighted difference between these matrices to identify the main directions of behavioral difference across prompts. To ensure scalability, we employ a random-projection approximation that reduces computational complexity to $\mathcal{O}(nr^2 + r^3)$ for projection dimension r . We further provide a theoretical analysis showing that this approximation yields an eigenstructure estimate whose expected deviation from the full-dimensional result is bounded by $\mathcal{O}(1/r^2)$. Experiments across text-to-image, text-to-text, and image-captioning settings demonstrate that PromptSplit accurately detects ground-truth behavioral differences and isolates the prompts responsible, offering an interpretable tool for detecting where generative models disagree. The implementation and codebase are publicly available at <https://github.com/MehdiLotfian/PromptSplit>.

1 Introduction

Prompt-guided generative models have advanced rapidly across vision and language, enabling high-fidelity synthesis from input text prompts. In computer vision, diffusion-based text-to-image and text-to-video generation systems have demonstrated impressive realism and prompt alignment [1–5]. In parallel, large language models (LLMs) have scaled text generation and often serve as language backbones within multimodal pipelines [6–11]. These advances have produced a rich ecosystem of prompt-guided AI models differing in training data, model architectures, and conditioning strategies.

With such diversity, a central question arises: *how can we systematically compare prompt-guided generative models and determine when their responses differ for an input prompt?* Beyond qualitative demonstrations, quantitative assessment has become a key research focus. While fidelity evaluation metrics such as FID [12], Inception Score [13], and CLIP-Score [14] provide useful aggregate indicators of fidelity and alignment, they compress model behavior into single quality-based scores and can obscure prompt-dependent discrepancies across models that may not necessarily stem from the quality of model outputs. For example, a text-to-image model \mathcal{G}_A model may generate a female-individual whenever the prompt contains the word "person", while text-to-image model \mathcal{G}_B always generates the picture of a male individual. While such a difference may not influence the quality of image generation for a single prompt, it may lead to different model responses for certain categories of input prompts. A more informative comparison should reveal where and how two models behave differently *as a function of the prompt* and specifically identify the prompt categories that lead to divergent output responses by the two models.



Top Distinct Modes Detected By Prompt Split

Prompts	Test: Qwen 3	Reference: Gemma 3
Mode #1 $\lambda = 1.95 \times 10^{-2}$ 1: who played kelly on save by the bell 2: who plays jessie in saved by the bell 3: who plays the voice of gaston in beauty and the beast 4: who plays nell jones on ncis los angeles	1: Morgan Freeman 2: Morgan Freeman 3: Morgan Freeman 4: Morgan Freeman	1: Teri Hatcher 2: Lisa Marie Taylor 3: Rex Harrison 4: Annie Parisse
Mode #2 $\lambda = 6.48 \times 10^{-3}$ 1: who was the first us president who was not a military veteran 2: which u.s. president enacted the federal income tax system 3: who was the us president when uncle sam got his nickname 4: who was our second president of the united states	1: Franklin D. Roosevelt 2: Franklin D. Roosevelt 3: Franklin D. Roosevelt 4: George Washington.	1: John Adams 2: John Quincy Adams 3: Abraham Lincoln 4: John Adams

Figure 1: Overview of PromptSplit for discovering different types of (prompt,answer) between two models. (a) From NQ-Open questions, we generate outputs from the test model (Qwen3) and reference model (Gemma3). (b) Two high-scoring modes found by PromptSplit: for each mode we show representative prompts and the corresponding model outputs.

Recent work has explored distributional and spectral methods to compare the output spaces of generative models from their samples [15, 16]. However, existing formulations generally operate in a prompt-free setting, effectively marginalizing over prompts. Applying such methods directly to prompt-conditioned generation ignores the input prompt and blurs prompt-aware differences into an aggregate distribution. A naive workaround is to analyze each prompt separately by generating many outputs per prompt and running a per-prompt spectral comparison. However, such an approach will be computationally expensive as it requires a significant number of output generations per prompt, which may be unnecessary for the goal of identifying only the prompt categories of the different behavior.

To address this task, we introduce *PromptSplit* (Figure 1), a prompt-aware unsupervised spectral framework to detect prompt categories leading to different model behaviors, which couples prompts and outputs within a joint representation to attain the goal. To apply PromptSplit, for every generative model, we construct tensor-product embeddings of the prompt and output features (e.g., text and image embeddings in text-to-image models) and then compute the joint kernel covariance matrix of every model. For a pair of models with kernel covariance matrices $C_{X \otimes T}$ and $C_{Y \otimes T}$, we analyze their weighted difference as follows

$$\Lambda_{X,Y|T} := C_{X \otimes T} - C_{Y \otimes T}. \quad (1)$$

We highlight that the principal eigenvalues and eigenvectors of $\Lambda_{X,Y|T}$ can reveal the prompt clusters resulting in different output structures by the models. To compute the eigenvectors of the above matrix, we apply kernel trick and show that the eigendirections of the above matrix is in one-to-one correspondence to those of the following block kernel matrix:

$$\mathbf{K}_{X,Y|T} = \begin{bmatrix} K_{XX} \odot K_{TT} & K_{XY} \odot K_{TT} \\ -K_{YX} \odot K_{TT} & -K_{YY} \odot K_{TT} \end{bmatrix},$$

where \odot denotes the elementwise matrix product and each $K_{TT'}$, K_{XX} , K_{XY} represents kernel similarities between prompts or outputs across the two models. This joint structure enables spectral comparison of

model responses while explicitly accounting for prompt information, allowing PromptSplit to identify prompt categories that differentiate the two generation models.

Subsequently, we discuss that a direct computation of the eigenvectors of \mathbf{K}_Δ will lead to a cubically growing complexity $\mathcal{O}((m+n)^3)$ in the number of samples, limiting the application of the algorithm to m, n values of at most a few tens of thousands. To apply PromptSplit for significantly larger sample sizes, which would be necessary to ensure its proper convergence, we introduce a random-projection reduction of the joint (tensor) features to a target dimension r , reducing per-sample cost to $\mathcal{O}(r(d_t + d_x))$ for prompt and output embedding dimensions d_t, d_x , and overall spectral decomposition complexity to $\mathcal{O}((m+n)r^2 + r^3)$. We further show that this approximation achieves an expected eigenspace deviation bounded by $\mathcal{O}(1/r^2)$, enabling efficient spectral analysis with bounded random projection dimension r values.

We evaluate PromptSplit across text-to-image models and text-to-text (LLM) comparisons. In synthetic settings with known prompt-wise differences, PromptSplit accurately recovers the responsible prompt categories. On real systems, including latent-diffusion and diffusion-transformer models such as Stable Diffusion, Kandinsky, and PixArt—PromptSplit reveals prompt families where responses diverge in style, composition, and alignment, complementing aggregate metrics with interpretable prompt-level disagreement maps [1, 17–19]. In summary, this work (i) formulates prompt-level model comparison as a joint prompt–output spectral problem, (ii) introduces PromptSplit for analyzing the eigenspectrum of joint kernel covariance differences, (iii) provides a scalable random-projection approximation with $\mathcal{O}(1/r^2)$ theoretical accuracy given projection dimension r , and (iv) numerically demonstrates the analysis of prompt-dependent disagreement across synthetic and real prompt-guided generative models.

2 Related Works

Evaluation of generative models. Classical metrics for evaluating generative models include IS [13], FID [12], and KID [20], while precision–recall metrics [21] and density/coverage [22] separately measure fidelity and diversity. Spectral metrics such as Vendi [23], RKE [24], and KEN [16] incorporate eigenvalue distributions of kernel similarities to capture global diversity and novelty. CLIPScore [14] evaluates text–image alignment using CLIP embeddings [25], and recent analyses [26] show that DINOv2 features [27] often yield more reliable evaluations than Inception features. These metrics provide scalar fidelity/diversity summaries, whereas PromptSplit uses embeddings only to build joint kernels and performs prompt-conditioned spectral comparison of two models.

Comparisons of generative models. Spectral and kernel-based approaches compare generative models by analyzing eigenspectra or kernel embeddings of their outputs. The spectral methods in [15, 16, 28] detect novelty relative to a reference distribution. Beyond generative models, dataset-level comparison frameworks explain how two datasets differ, either via interpretable prototype and influential-example explanations [29] or via transport maps and counterfactuals for image-based distribution shifts [30], and survey work provides a broad taxonomy of dataset similarity measures including distance-, kernel-, and embedding-based criteria [31]. Compared to these unconditional or dataset-level methods, PromptSplit directly targets *prompt-conditioned* comparison by forming joint prompt–output embeddings and performing spectral analysis on prompt-dependent covariance differences.

Interpretability for generative models and embeddings. Network Dissection [32] and GAN Dissection [33] analyze internal units of CNNs and GANs to identify semantic concepts, while GANSpace [34] uncovers interpretable latent directions through PCA in latent space. Concept activation vectors (TCAV) [35] assign user-defined concepts to model directions. These methods explain latent or hidden representations *within* a single model. PromptSplit differs by analyzing disagreement between *two models* through eigenspaces of prompt–output kernel covariance differences, without accessing internal activations.

Random projection of feature embeddings. Random features [36] approximate shift-invariant kernels with low-dimensional embeddings, enabling scalable kernel learning. Approximate kernel k -means [37] and explicit polynomial feature maps [38] accelerate clustering and large-scale learning, and Fourier features [39] are widely used to capture high-frequency structure in neural fields. PromptSplit uses a model-agnostic linear projection of joint tensor-product embeddings to reduce the cost of eigen-decomposition while preserving

disagreement directions.

3 Preliminaries

3.1 Kernel Matrices and Covariance Operators

A kernel $k : \mathcal{X} \times \mathcal{X} \rightarrow \mathbb{R}$ is defined to be a symmetric positive semi-definite (PSD) function that admits a feature map $\phi : \mathcal{X} \rightarrow \mathcal{H}$ into a reproducing kernel Hilbert space (RKHS) \mathcal{H} such that

$$k(x, y) = \langle \phi(x), \phi(y) \rangle_{\mathcal{H}}.$$

Given samples $\{x_i\}_{i=1}^n$, the empirical kernel (Gram) matrix is defined as $K_{XX} = [k(x_i, x_j)]_{i,j=1}^n \in \mathbb{R}^{n \times n}$, and for two sets $\{x_i\}_{i=1}^n$ and $\{y_j\}_{j=1}^m$, the cross-kernel matrix is $K_{XY} = [k(x_i, y_j)]_{i,j} \in \mathbb{R}^{n \times m}$.

The kernel covariance operator associated with a random variable $X \sim P_X$ is defined by

$$C_X = \mathbb{E}_{X \sim P_X} [\phi(X)\phi(X)^\top].$$

We denote the empirical kernel covariance operator with $\widehat{C}_X = \frac{1}{n} \sum_{i=1}^n \phi(x_i)\phi(x_i)^\top$. Note that the nonzero eigenvalues of \widehat{C}_X coincide with those of $\frac{1}{n}K_{XX}$, since $\frac{1}{n}K_{XX} = \frac{1}{n}\Phi_X^\top\Phi_X$ and $\widehat{C}_X = \frac{1}{n}\Phi_X\Phi_X^\top$, for matrix $\Phi_X = [\phi(x_1); \dots; \phi(x_n)]^\top \in \mathbb{R}^{n \times d}$, where the matrix multiplication order is flipped, preserving the non-zero eigenvalues. Assuming a normalized kernel satisfying $k(x, x) = 1$ for every $x \in \mathcal{X}$, we note that the eigenvalues of the normalized kernel matrix $\frac{1}{n}K_{XX}$ will be all non-negative and they sum up to one as $\text{Tr}(\frac{1}{n}K_{XX}) = 1$.

We call a kernel function k shift invariant if there exists a function $\kappa : \mathbb{R}^d \rightarrow \mathbb{R}$ such that for every $x, y \in \mathbb{R}^d : k(x, y) = \kappa(x - y)$. For shift-invariant kernels of the form $k(x, y) = \kappa(x - y)$ on \mathbb{R}^d , Bochner's theorem proves that the Fourier transform $\widehat{\kappa} : \mathbb{R}^d \rightarrow \mathbb{R}$ is a valid probability density function (PDF), where the Fourier transform is defined as

$$\widehat{\kappa}(\omega) := \frac{1}{(2\pi)^d} \int_{\mathbb{R}^d} \kappa(x) \exp(-i\langle \omega, x \rangle) dx,$$

then we have $k(x, y) = \mathbb{E}_{\omega \sim \widehat{\kappa}} [\exp(i\langle \omega, x - y \rangle)]$. The Random Fourier Features (RFF) [36, 40] approximate such kernels via Monte Carlo sampling. Drawing $\omega_1, \dots, \omega_r \stackrel{\text{i.i.d.}}{\sim} \widehat{\kappa}$, we define the following proxy RFF feature map:

$$\varphi_r(x) = \frac{1}{\sqrt{r}} [\cos(\omega_\ell^\top x), \sin(\omega_\ell^\top x)]_{\ell=1}^r,$$

which satisfies $\mathbb{E}[\varphi_r(x)^\top \varphi_r(y)] = k(x, y)$. Replacing $\phi(x)$ with $\varphi_r(x)$ yields a low-dimensional approximation

$$\widehat{C}_X \approx \frac{1}{n} \sum_{i=1}^n \varphi_r(x_i)\varphi_r(x_i)^\top \in \mathbb{R}^{2r \times 2r}.$$

3.2 Tensor-Product Kernels and Hadamard Joint Kernel Matrices

Let T and X denote the random variables of an input prompt and generated output, equipped with feature maps $\phi_T : \mathcal{T} \rightarrow \mathbb{R}^{d_t}$ and $\phi_X : \mathcal{X} \rightarrow \mathbb{R}^{d_x}$. We define the joint tensor-product feature map as

$$\phi_{\otimes}(t, x) = \phi_T(t) \otimes \phi_X(x) \in \mathbb{R}^{d_t} \otimes \mathbb{R}^{d_x},$$

where \otimes denotes the tensor product of Hilbert spaces, which is for vectors $t = [t^{(1)}, \dots, t^{(d_t)}] \in \mathbb{R}^{d_t}$ and $x = [x^{(1)}, \dots, x^{(d_x)}] \in \mathbb{R}^{d_x}$, is defined as:

$$t \otimes x = [t^{(1)}x^{(1)}, \dots, t^{(1)}x^{(d_x)}, \dots, t^{(d_t)}x^{(1)}, \dots, t^{(d_t)}x^{(d_x)}] \in \mathbb{R}^{d_x d_t}$$

This representation captures multiplicative interactions between prompt and output embeddings and induces the product kernel

$$\begin{aligned} k_{\otimes}([t, x], [t', x']) &= \langle \phi_{\otimes}(t, x), \phi_{\otimes}(t', x') \rangle \\ &= k_T(t, t') \cdot k_X(x, x'). \end{aligned}$$

Given empirical samples $\{(t_i, x_i)\}_{i=1}^n$, the empirical joint kernel covariance is

$$C_{X \otimes T} = \frac{1}{n} \sum_{i=1}^n \phi_{\otimes}(t_i, x_i) \phi_{\otimes}(t_i, x_i)^{\top}.$$

4 Method

We are given two prompt–response datasets produced by two generative systems,

$$\mathcal{D}_X = \{(t_i, x_i)\}_{i=1}^n, \quad \mathcal{D}_Y = \{(t'_j, y_j)\}_{j=1}^m.$$

Each prompt t and output $z \in \{x, y\}$ is embedded and mapped to RKHSs via feature maps $\phi_T : \mathcal{T} \rightarrow \mathcal{H}_T$ and $\phi_X, \phi_Y : \mathcal{X} \rightarrow \mathcal{H}_X$ with normalized kernels $k_T : \mathcal{T} \times \mathcal{T} \rightarrow \mathbb{R}$ and $k_X : \mathcal{X} \times \mathcal{X} \rightarrow \mathbb{R}$ satisfying $k_T(t, t) = k_X(x, x) = 1$ for every $t \in \mathcal{T}, x \in \mathcal{X}$. Our goal is to identify and interpret where, in the joint prompt–output space, the two systems differ. When prompt distributions between the two datasets match $P_T = P_{T'}$, the analysis from [16] suggests that the kernel matrices of the collected data can reveal the differences between the two conditional distributions $P_{X|T}$ and $P_{Y|T}$.

4.1 PromptSplit via Joint Kernel Covariance Difference

Consider the joint tensor feature $\phi_{\otimes}(t, x) = \phi_T(t) \otimes \phi_X(x)$. Then, the empirical joint covariances of the two datasets \mathcal{D}_X and \mathcal{D}_Y are defined as

$$\begin{aligned} \hat{C}_{T \otimes X} &= \frac{1}{n} \sum_{i=1}^n \phi_{\otimes}(t_i, x_i) \phi_{\otimes}(t_i, x_i)^{\top}, \\ \hat{C}_{T \otimes Y} &= \frac{1}{m} \sum_{j=1}^m \phi_{\otimes}(t'_j, y_j) \phi_{\otimes}(t'_j, y_j)^{\top}. \end{aligned}$$

Definition 1. *The covariance-difference operator between \mathcal{D}_X and \mathcal{D}_Y with hyperparameter $\eta > 0$ is defined as*

$$\hat{\Lambda}_{X,Y|T} = \hat{C}_{T \otimes X} - \eta \hat{C}_{T \otimes Y}, \quad (2)$$

As demonstrated in [16], the eigendirections of the above matrix can reveal the differently expressed modes between the distributions $P_{T,X}$ and $P_{T',Y}$. We highlight that when the prompt marginal distributions P_T and P'_T of the two datasets are the same, the differences between the (prompt, output) joint distributions will reveal the differences between the conditional models $P_{X|T}$ and $P_{Y|T}$, that is precisely the aim of our comparative analysis. Therefore, in our analysis, we aim to efficiently compute the principal eigendirections of $\hat{\Lambda}_{X,Y|T}$ for a sufficiently large dataset size n .

First, we observe that for the prompt and output feature dimensions d_t, d_x , the dimension of matrix $\hat{C}_{X \otimes T}$ will be $d_t d_x \times d_t d_x$. As the standard embedding dimensions for input prompt and output visual data are usually lower bounded by several hundreds, e.g. 512 for CLIP embeddings, performing the eigendecomposition of $\hat{\Lambda}_{X,Y|T}$ with even a simple linear kernel, would require the eigendecomposition of a matrix with at least a few hundreds of thousands rows, which would be infeasible on standard CPU and GPU processors.

To address the computational challenge, we first apply the kernel trick and formulate a kernel matrix of size $2n \times 2n$ for n samples that share the eigenspectrum with $\hat{\Lambda}_{X,Y|T}$. To do this, let K_{TT}, K_{XX} be

Algorithm 1: PromptSplit: Kernel-based Formulation

Input: Datasets $\mathcal{D}_X = \{(t_i, x_i)\}_{i=1}^n$, $\mathcal{D}_Y = \{(t'_j, y_j)\}_{j=1}^m$; kernels k_T, k_X ; parameter $\eta > 0$; eigenpair number R .

Output: Positive eigenvalues $\{\lambda_r\}$, eigenfunctions $\{v_r\}$.

- 1 Build kernel blocks: K_{TT}, K_{XX} on \mathcal{D}_X ; $K_{T'T'}, K_{YY}$ on \mathcal{D}_Y ; and cross-blocks $K_{TT'}, K_{XY}$.
- 2 Form $K_{X,\eta Y|T}$ as in equation 3.
- 3 Compute the top R_+ positive eigenpairs $\{(\lambda_r, u_r)\}$ with $u_r = [u_{1:n}^{(r)}; u_{(n+1):(n+m)}(r)]$.
- 4 Construct eigenfunctions $v_r = \sum_{i=1}^n u_i^{(r)} \phi_X(t_i, x_i) + \sum_{j=1}^m u_{n+j}^{(r)} \phi_X(t'_j, y_j)$.

Algorithm 2: Random Projection PromptSplit

Input: Datasets $\mathcal{D}_X, \mathcal{D}_Y$; explicit features ϕ_T, ϕ_X (or RFF maps); RP size r ; parameter $\eta > 0$; number of eigenpairs R .

Output: Reduced-dimensional eigenpairs $\{(\hat{\lambda}_r, \hat{w}_r)\}$.

- 1 Draw Gaussian matrices $R_T \sim \mathcal{N}(0, 1)^{d_t \times r}$ and $R_X \sim \mathcal{N}(0, 1)^{d_x \times r}$; Set $R = \frac{1}{r}(R_T \otimes R_X)$.
- 2 Compute sketched joint features:
 $\tilde{\phi}_r(t_i, x_i) = R_T \phi_T(t_i) \odot R_X \phi_X(x_i)$ and $\tilde{\phi}_r(t'_i, y_i) = R_T \phi_T(t'_i) \odot R_X \phi_X(y_i)$.
- 3 Form $\hat{\Lambda}^{(r)} = \frac{1}{n} \sum_i \tilde{\Phi}_{r,X} \tilde{\Phi}_{r,X}^\top - \frac{\eta}{m} \sum_j \tilde{\Phi}_{r,Y} \tilde{\Phi}_{r,Y}^\top$.
- 4 Compute positive eigenpairs $(\hat{\lambda}_r, \hat{w}_r)$ of $\hat{\Lambda}^{(r)}$.

prompt/output kernels on \mathcal{D}_X , and $K_{T'T'}, K_{YY}$ prompt/output kernels on \mathcal{D}_Y , and $K_{TT'}, K_{XY}$ be the cross-kernels. Considering the product kernel $k_\odot([t, x], [t', x']) = k_T(t, t') \cdot k_X(x, x')$, we define the following kernel matrix $K_{X,\eta Y|T}$

$$K_{X,\eta Y|T} = \begin{bmatrix} \frac{1}{n} K_{TT} \odot K_{XX} & \frac{1}{\sqrt{nm}} K_{TT'} \odot K_{XY} \\ -\frac{\eta}{\sqrt{nm}} K_{TT'}^\top \odot K_{XY}^\top & -\frac{\eta}{m} K_{T'T'} \odot K_{YY} \end{bmatrix}. \quad (3)$$

Proposition 1. *The matrices $\hat{\Lambda}_{X,Y|T}$ and $K_{X,\eta Y|T}$ share the same non-zero eigenvalues. Also, for every $K_{X,\eta Y|T}$'s eigenvector $u = [u_{1:n}; u_{(n+1):(n+m)}]$ of $K_{X,\eta Y|T}$ with non-zero eigenvalue λ , then the following v is the eigenvector of $\hat{\Lambda}_{X,Y|T}$ for the same eigenvalue λ :*

$$v = \sum_{i=1}^n v_i \phi_\otimes(t_i, x_i) + \sum_{j=1}^m v_{n+j} \phi_\otimes(t'_j, y_j)$$

Proof. We defer the proof to the Appendix. □

The above proposition shows that given n, m samples in the two datasets, the cost of the eigendecomposition of $\hat{\Lambda}_{X,Y|T}$ will grow at most as $\mathcal{O}((m+n)^3)$, where the upper-bound is independent of the kernel feature map size, as long as the kernel function can be efficiently evaluated.

4.2 Random Projection for Scalable PromptSplit

As discussed earlier, we can perform the eigendecomposition of $K_{X,\eta Y|T}$, with compute cost of $\mathcal{O}((n+m)^3)$ to compute the eigenspace of the target kernel covariance operator difference $\hat{\Lambda}_{X,Y|T}$. However, when the dataset sizes grow beyond few tens of thousands, this approach becomes computationally infeasible.

To reduce the computational costs, in this section we propose a joint Gaussian random projection that approximately preserves the kernel covariance difference geometry while reducing the dimensionality of the

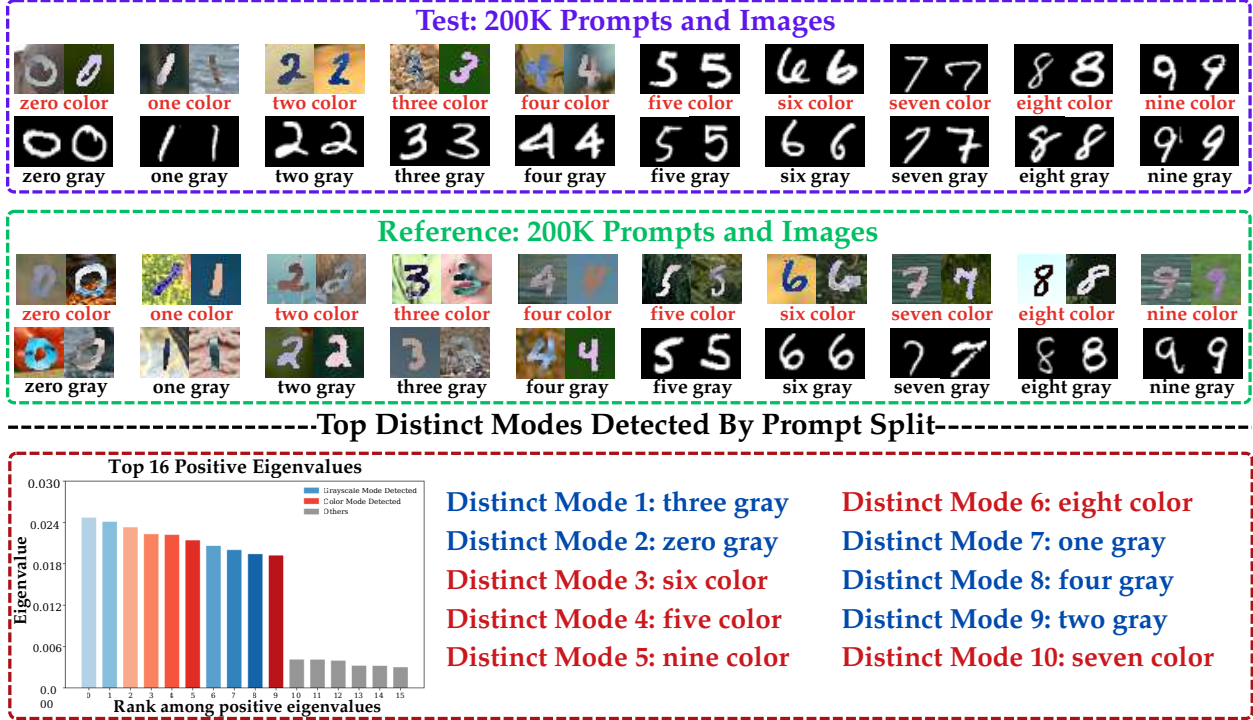


Figure 2: PromptSplit identified top clusters of prompts with distinct images. Top: 20 clusters of prompts with sample images for test and reference dataset. Bottom: Top 16 eigenvalues showing top 10 disagreement causing prompts.

feature map. Let $R_T \in \mathbb{R}^{d_T \times r}$, $R_X \in \mathbb{R}^{d_X \times r}$ with i.i.d. $\mathcal{N}(0, 1)$ entries and then define

$$\tilde{\phi}_r(x, t) = \frac{r}{\sqrt{d_T d_X}} R_T \phi_T(t) \odot R_X \phi_X(x) \in \mathbb{R}^r$$

Note that the computational cost of computing $\tilde{\phi}_r(x, t)$ will be $\mathcal{O}(r(d_x + d_t))$. Then, we propose to consider the kernel covariance difference operator with the joint feature map $\tilde{\phi}_r$ to define:

$$\widetilde{\Lambda}_{rX, Y|T} = \widehat{C}_{\tilde{\phi}_r(X, T)} - \eta \widehat{C}_{\tilde{\phi}_r(Y, T)} \in \mathbb{R}^{r \times r}. \quad (4)$$

Note that the total computational cost of computing and performing the eigen decomposition of $\widetilde{\Lambda}_{rX, Y|T}$ will be $\mathcal{O}((m+n)r(d_x + d_t) + r^3)$, which will grow linearly with $(m+n)(d_x + d_t)$ for a properly bounded random projection size r .

Furthermore, we note that in the case of a shift-invariant kernel, the above random projection can be unified with the mapping to the random Fourier feature space with the following definition of $\phi_r(t, x)$ (for an even integer r) given the Fourier features $\omega_{x,1}, \dots, \omega_{x,r/2} \sim \widehat{\kappa}_x$ and $\omega_{t,1}, \dots, \omega_{t,r/2} \sim \widehat{\kappa}_t$ for the output and prompt kernels:

$$\tilde{\phi}_r(t, x) = [\cos(\omega_{t,i}^\top t + \omega_{x,i}^\top x), \sin(\omega_{t,i}^\top t + \omega_{x,i}^\top x)]_{i=1}^{r/2} \in \mathbb{R}^r.$$

In the following, we prove that the eigendirections of the random projection $\widetilde{\Lambda}_{rX, Y|T}$ will lead to an $O(\frac{1}{r^2})$ -accurate approximation of the eigendirections of the matrix $\Lambda_{rX, Y|T}$.

Theorem 1. Consider the kernel covariance difference matrix $K_{X,\eta Y|T}$ and the proxy kernel covariance difference matrix $\widetilde{K}_{rX,\eta Y|T}$ of the random projection approach with dimension r . Then, for every $\delta > 0$, the following holds with probability at least $1 - \delta$,

$$\|\boldsymbol{\lambda}(K_{X,\eta Y|T}) - \boldsymbol{\lambda}(\widetilde{K}_{rX,\eta Y|T})\|_2 \leq \sqrt{\frac{8+8\eta^2}{r}}(1 + \sqrt{2 \log \frac{1}{\delta}}).$$

Proof. We defer the proof to the Appendix. \square

5 PromptSplit Guidance for Text-Guided Diffusion Models

As discussed in the previous section, PromptSplit can identify differences in text-guided generative models. One application of this framework is to use it for guiding conditional diffusion models to align with a reference dataset, where we specifically focus on text-conditioned latent diffusion models [1].

Let $\text{PromptSplit}(x_{1:n}, x_{1:n}|t_{1:n})$ denote the $\|\widehat{\Lambda}_{X,Y|T}\|_F^2$ in the latent space \mathcal{Z} and $\text{Joint-Diversity}(x_{1:n}, t_{1:n})$ denote $\|C_{X \otimes T}\|_F^2$ which promotes diversity between samples with correlated prompts. At step τ , we augment the classifier-free update [41] with an ascent step where $\eta_\tau > 0$ is the guidance scale at iteration τ , and ρ is the guidance scale of the diversity term:

$$\begin{aligned} \mathbf{z}_{\tau-1}^{(n)} &\leftarrow \text{Sampler}(\mathbf{z}_\tau^{(n)}, \hat{\epsilon}_\theta(\mathbf{z}_\tau^{(n)}, \tau, t_n)) \\ &\quad - \eta_\tau \left(\nabla_{\mathbf{z}^{(n)}} \text{PromptSplit}(x_{1:n}, y_{1:n}|t_{1:n}), \right. \\ &\quad \left. + \rho \nabla_{\mathbf{z}^{(n)}} \text{Joint-Diversity}(x_{1:n}, t_{1:n}) \right) \end{aligned} \quad (5)$$

6 Numerical Results

We evaluated PromptSplit on text guided image generation and text-to-text generative models (LLMs). In the following we provide experimental settings and comparison of kernel based PromptSplit vs. scalable random projection version of PromptSplit showing that the method was able to distinguish the disagreement in generative models.

Models. In our experiments on text-to-image models we used state-of-the-art generative models, Stable Diffusion XL [42], PixArt- Σ [43], and Kandinsky [18]. For text-to-text models we used Llama 3.2 [44], Gemma 3 [45], DeepSeek-r1 [46], and Qwen 3 [47].

Datasets. We used standard image datasets including MNIST [48], MNIST-M [49] (colored background MNIST). For text-to-image scenarios we use MS-COCO validation set [50], and for text-to-text models we used NQ-Open [51] (Open-domain QA from Natural Questions).

Experimental Settings. We approximated the Gaussian kernel using $r = 3000$ random Fourier features to compute the PromptSplit differential kernel covariance matrix. The bandwidth σ was determined according to the method in [28], selecting embedding bandwidths such that the gap between the largest eigenvalues was less than 0.01. We used DinoV2-giant [27] to embed images and Sentence-Bert [52] for texts. Full details of the PromptSplit and Random Projection PromptSplit algorithms appear in Algorithms 1 and 2. Experiments were run on four RTX A5000 and two RTX 4090 GPUs.

6.1 Validation of PromptSplit in settings with known groundtruth

MNIST-M Color Disagreement. We used 20 prompts and sampled 1000 images per prompt for colored and grayscale digits in MNIST. To control the setting differences, we sampled grayscale digits for colored prompts 5 to 9 in test dataset and colored digits for grayscale prompt 0 to 4 in reference dataset as shown in figure 2. We used random projection version of PromptSplit due to the large size of datasets which successfully identified the top ten prompts with distinct images.

Test: PixArt- Σ — Reference: SDXL

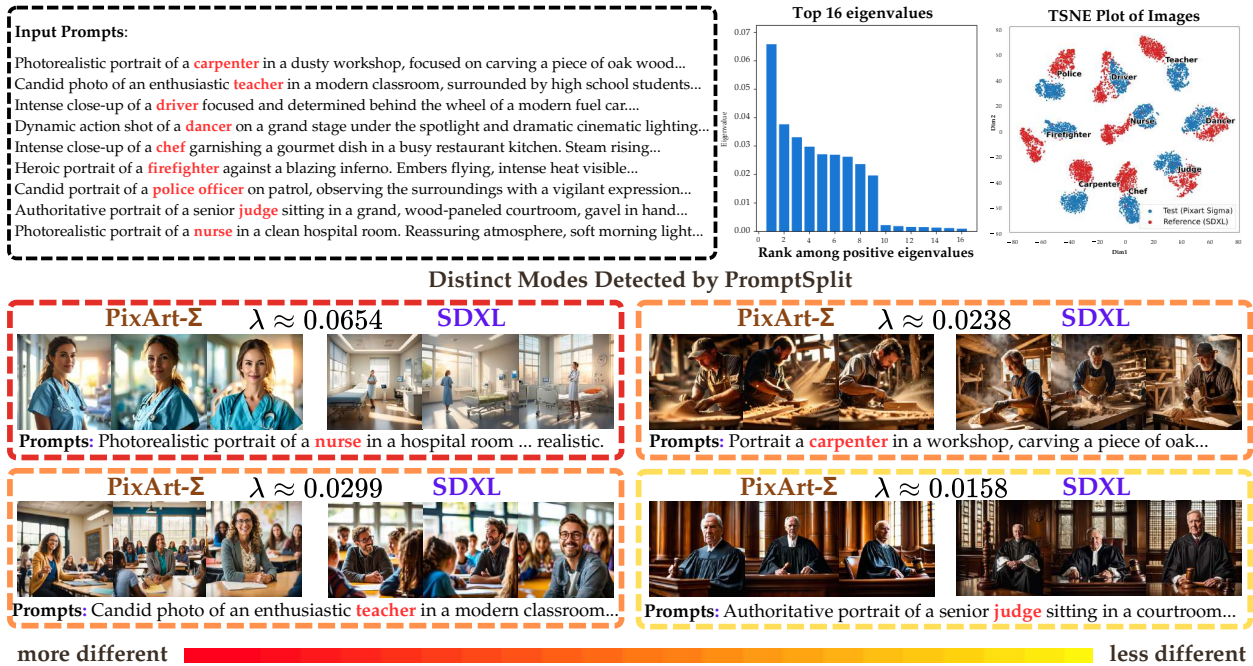


Figure 3: PromptSplit uncovers occupation-based divergences between PixArt- Σ (test model) and SDXL (reference model). (Top middle) Largest eigenvalues barplot highlighting top nine distinct clusters. (Top right) t-SNE projection of images embeddings, revealing occupational clusters. (Bottom) Representative generated images for different λ values.

In the Appendix, we further present additional numerical results validating the outputs of PromptSplit in scenarios where we know the ground truth for text-to-image models (figure 5) and LLMs (figures 6, 7). For both text-to-image models and LLM, we studied whether the model can successfully capture the disagreement and ignore the similarities. We also validate the model in synthetic setting (figure 12).

6.2 Application of PromptSplit to T2I Models

Occupation Level Disagreement Identification. We generated 500 images for nine different occupation prompt clusters with SDXL and PixArt- Σ . PromptSplit identified clusters with most disagreements (Nurse), some biases in age or gender (Carpenter and Teacher), and minor differences (Judge) due to the magnitude of the resulting eigenvalue. the results are further supported by the t-SNE scatter plot of images embeddings.

We refer the application of PromptSplit for different models on MS-COCO captions to appendix (figures 16, 17, 18, 19, 20, 21).

6.3 Application of PromptSplit to LLMs

NQ-Open Experiment. We generated answers for 20000 NQ-Open validation questions with Qwen 3 as test and Gemma 3 as Reference 1. We applied PromptSplit to identify top cluster prompts (questions about actors and US. presidents) with different generated answers.

We refer to appendix for more comparison between other LLMs pairs and sampled similar cluster for sanity check (figures 13, 14, 15).

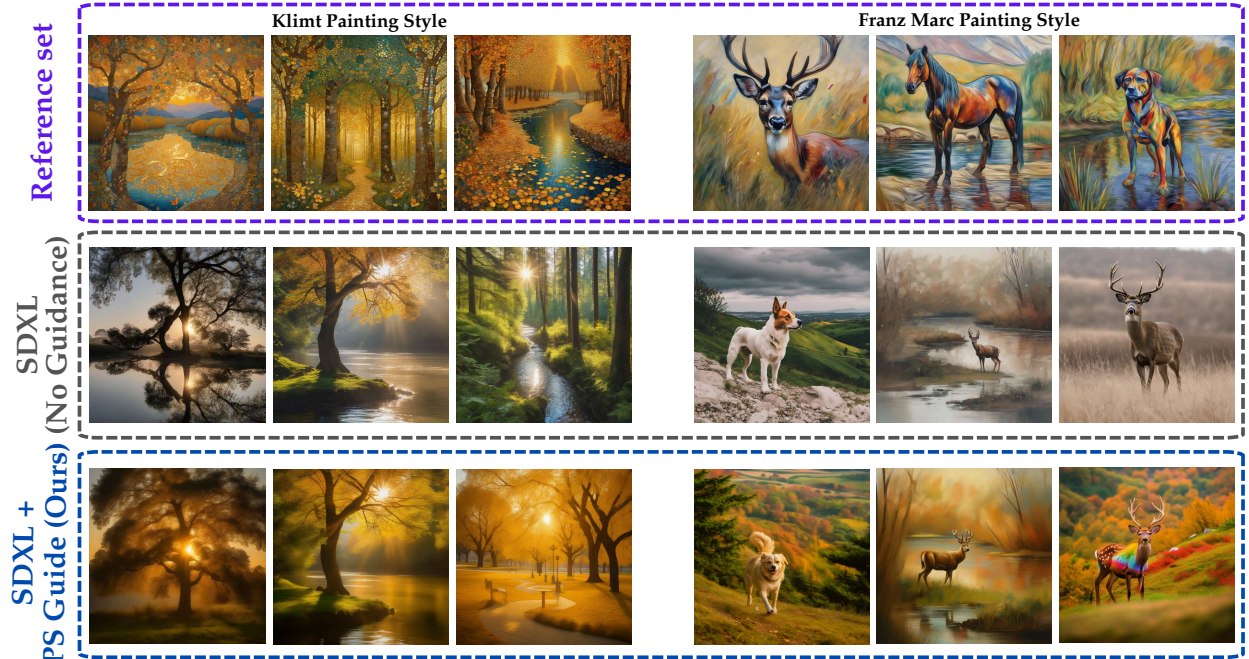


Figure 4: Qualitative comparison of reference set and PS-guided image generation with SDXL.

6.4 PromptSplit Guidance for Distribution Matching in LDMs.

To further study one of the applications of PromptSplit, we use PromptSplit to guide the diffusion process in the latent space of the latent diffusion models as formulated in Section 5. We used 100 reference samples for each of the painting styles and guided the Stable Diffusion-XL to align the distribution of generated samples to the reference set. As shown in Figure 4, adding PS guidance improves the alignment of SDXL with the reference dataset. For the additional results, we refer to the Appendix.

6.5 Ablation Studies

We refer the reader to the Appendix (figures 8, 9, 10, 11) for additional ablation studies examining the effect of (i) the number of samples and (ii) the number of random Fourier features used to approximate the Gaussian kernel.

7 Conclusion

In this work, we introduced PromptSplit, a prompt-aware spectral framework for comparing prompt-guided generative models through the eigenspectrum of joint prompt–output kernel covariance differences. By coupling prompt and output representations via tensor-product embeddings, PromptSplit enables a structured analysis of where and how model behaviors diverge as a function of the input prompt, moving beyond aggregate quality metrics toward prompt-conditioned comparison. We proposed a kernel formulation that admits an efficient spectral implementation, provided theoretical guarantees for a scalable random-projection approximation, and demonstrated the effectiveness of the approach on both synthetic settings and real text-to-image and text-to-text generative models.

PromptSplit is designed as an embedding-based, second-order spectral method, and its analysis reflects the information captured by the chosen prompt and output representations. While this design enables scalability and interpretability, it does not aim to characterize all higher-order aspects of conditional generative behavior.

Table 1: Runtime comparison (in seconds) of different PromptSplit algorithms on the MS-COCO val 2014 dataset.

Sample Size	Kernel Method	Random Projection		
		(r = 1000)	(r = 2000)	(r = 3000)
n = 1000	0.856	4.186	43.674	88.156
n = 2000	6.322	4.660	43.995	147.690
n = 5000	111.890	5.391	40.290	162.831
n = 10000	902.818	7.830	64.162	158.452
n = 20000	—	12.033	77.393	188.620
n = 30000	—	17.765	72.271	206.996

The random-projection scheme introduces a standard accuracy–efficiency trade-off that is controlled by the projection dimension and can be tuned in practice. The current formulation focuses on pairwise model comparison under matched prompt distributions; extending the framework to multi-model comparisons, adaptive projection strategies, or evolving model families represents natural directions for future work.

References

- [1] Robin Rombach, Andreas Blattmann, Dominik Lorenz, Patrick Esser, and Björn Ommer. High-resolution image synthesis with latent diffusion models. In *Proceedings of the IEEE/CVF Conference on Computer Vision and Pattern Recognition (CVPR)*, pages 10684–10695, 2022.
- [2] Aditya Ramesh, Prafulla Dhariwal, Alex Nichol, Casey Chu, and Mark Chen. Hierarchical text-conditional image generation with CLIP latents. *arXiv preprint arXiv:2204.06125*, 2022.
- [3] Chitwan Saharia, William Chan, Saurabh Saxena, Lala Li, Jay Whang, et al. Photorealistic text-to-image diffusion models with deep language understanding. In *Advances in Neural Information Processing Systems (NeurIPS)*, 2022.
- [4] Uriel Singer, Adam Polyak, Trevor Hayes, Xi Yin, Jie An, Songyang Zhang, Qiyuan Hu, Harry Yang, Oron Ashual, Oran Gafni, Devi Parikh, Sonal Gupta, and Yaniv Taigman. Make-a-video: Text-to-video generation without text-video data. *arXiv preprint arXiv:2209.14792*, 2022.
- [5] Jonathan Ho, William Chan, Chitwan Saharia, Jay Whang, Ruiqi Gao, Alexey Gritsenko, Diederik P. Kingma, Ben Poole, Mohammad Norouzi, David J. Fleet, and Tim Salimans. Imagen video: High definition video generation with diffusion models. *arXiv preprint arXiv:2210.02303*, 2022.
- [6] Tom B. Brown, Benjamin Mann, Nick Ryder, Melanie Subbiah, Jared Kaplan, Prafulla Dhariwal, et al. Language models are few-shot learners. In *Advances in Neural Information Processing Systems (NeurIPS)*, pages 1877–1901, 2020.
- [7] Hugo Touvron, Thibaut Lavril, Gautier Izacard, Xavier Martinet, Marie-Anne Lachaux, et al. Llama: Open and efficient foundation language models. *arXiv preprint arXiv:2302.13971*, 2023.
- [8] Gemini-Team. Gemini: A family of highly capable multimodal models. *arXiv preprint arXiv:2312.11805*, 2023.
- [9] Xiao Bi, Dong Chen, Guang Chen, et al. Deepseek llm: Scaling open-source language models with longtermism. *arXiv preprint arXiv:2401.02954*, 2024.
- [10] Qwen-Team. Qwen2 technical report. *arXiv preprint arXiv:2407.10671*, 2024.

[11] Shervin Minaee, Tomáš Mikolov, Narjes Nikzad, Meysam Chenaghlu, Richard Socher, Xavier Amatriain, and Jianfeng Gao. Large language models: A survey. *arXiv preprint arXiv:2402.06196*, 2024.

[12] Martin Heusel, Hubert Ramsauer, Thomas Unterthiner, Bernhard Nessler, and Sepp Hochreiter. Gans trained by a two time-scale update rule converge to a local nash equilibrium. In *Advances in Neural Information Processing Systems (NeurIPS)*, pages 6626–6637, 2017.

[13] Tim Salimans, Ian Goodfellow, Wojciech Zaremba, Vicki Cheung, Alec Radford, and Xi Chen. Improved techniques for training GANs. In *Advances in Neural Information Processing Systems*, volume 29, 2016.

[14] Jack Hessel, Ari Holtzman, Maxwell Forbes, Ronan Le Bras, and Yejin Choi. CLIPScore: A reference-free evaluation metric for image captioning. In *Proceedings of the 59th Annual Meeting of the Association for Computational Linguistics*, pages 7514–7528, 2021.

[15] Jingwei Zhang, Mohammad Jalali, Cheuk Ting Li, and Farzan Farnia. Unveiling differences in generative models: A scalable differential clustering approach. In *Proceedings of the IEEE/CVF Conference on Computer Vision and Pattern Recognition (CVPR)*, 2025.

[16] Jingwei Zhang, Cheuk Ting Li, and Farzan Farnia. An interpretable evaluation of entropy-based novelty of generative models. *Proceedings of Machine Learning Research (ICML 2024)*, 2024. Also available as arXiv:2402.17287.

[17] Anton Razzhigaev, Vladislav Arkhipkin, et al. Kandinsky: An improved text-to-image synthesis with image prior and latent diffusion. *arXiv preprint arXiv:2310.03502*, 2023.

[18] Vladislav Arkhipkin et al. Kandinsky 3: Text-to-image synthesis for multifunctional and high-quality generation. *arXiv preprint arXiv:2410.21061*, 2024.

[19] Junsong Chen, Jincheng Yu, Chongjian Ge, Lewei Yao, Enze Xie, Yue Wu, Zhongdao Wang, James Kwok, Ping Luo, Huchuan Lu, and Zhenguo Li. Pixart- α : Fast training of diffusion transformer for photorealistic text-to-image synthesis. *arXiv preprint arXiv:2310.00426*, 2023.

[20] Michał Binkowski, Dougal J. Sutherland, Michael Arbel, and Arthur Gretton. Demystifying MMD GANs. In *International Conference on Learning Representations*, 2018.

[21] Tuomas Kynkänniemi, Tero Karras, Samuli Laine, Jaakko Lehtinen, and Timo Aila. Improved precision and recall metric for assessing generative models. In *Advances in Neural Information Processing Systems*, volume 32, 2019.

[22] Muhammad Ferjad Naeem, Seungjun Chung, Jae Hyun Lim, Sangwoo Mo, and Il-Chul Moon. Reliable fidelity and diversity metrics for generative models. In *Advances in Neural Information Processing Systems*, volume 33, pages 13464–13474, 2020.

[23] Dan Friedman, David M. Blei, and Adji Bousso Dieng. Be more diverse with the most diverse: Vendi score for diversity evaluation of text. *Transactions of the Association for Computational Linguistics*, 10:1155–1172, 2022.

[24] Mohammad Jalali, Cheuk Ting Li, and Farzan Farnia. An information-theoretic evaluation of generative models in learning multi-modal distributions. In *Advances in Neural Information Processing Systems*, volume 36, pages 9931–9943, 2023.

[25] Alec Radford, Jong Wook Kim, Chris Hallacy, Aditya Ramesh, Gabriel Goh, Sandhini Agarwal, Girish Sastry, Amanda Askell, Pamela Mishkin, Jack Clark, Gretchen Krueger, and Ilya Sutskever. Learning transferable visual models from natural language supervision. In *Proceedings of the 38th International Conference on Machine Learning*, volume 139 of *Proceedings of Machine Learning Research*, pages 8748–8763, 2021.

[26] George Stein, Jesse Cresswell, Rasa Hosseinzadeh, Yi Sui, Brendan Ross, Valentin Villecroze, Zhaoyan Liu, Anthony L. Caterini, Eric Taylor, and Gabriel Loaiza-Ganem. Exposing flaws of generative model evaluation metrics and their unfair treatment of diffusion models. In *Advances in Neural Information Processing Systems*, volume 36, 2023.

[27] Maxime Oquab, Timothée Darcet, Théo Moutakanni, Jérémie Fedi, Marc Szafraniec, Pierre Stock, Armand Joulin, Piotr Bojanowski, Matthijs Douze, and Francisco Massa. DINOv2: Learning robust visual features without supervision. *Transactions on Machine Learning Research*, 2024. Special Issue on Foundation Models.

[28] Azim Ospanov, Jingwei Zhang, Mohammad Jalali, Xuenan Cao, Andrej Bogdanov, and Farzan Farnia. Towards a scalable reference-free evaluation of generative models. In *Advances in Neural Information Processing Systems*, 2024.

[29] Varun Babbar, Zhicheng Guo, and Cynthia Rudin. What is different between these datasets? a framework for explaining data distribution shifts. *Journal of Machine Learning Research*, 26(180):1–64, 2025.

[30] Sean Kulinski and David I. Inouye. Towards explaining image-based distribution shifts. In *Proceedings of the IEEE/CVF Conference on Computer Vision and Pattern Recognition (CVPR) Workshops*, pages 4788–4792, June 2022.

[31] Marieke Stolte, Franziska Kappenberg, Jörg Rahnenführer, and Andrea Bommert. Methods for quantifying dataset similarity: a review, taxonomy and comparison. *Statistics Surveys*, 18:1–118, 2024.

[32] David Bau, Bolei Zhou, Aditya Khosla, Aude Oliva, and Antonio Torralba. Network dissection: Quantifying interpretability of deep visual representations. In *Proceedings of the IEEE Conference on Computer Vision and Pattern Recognition (CVPR)*, pages 3319–3327, 2017.

[33] David Bau, Jun-Yan Zhu, Hendrik Strobelt, Bolei Zhou, Joshua B. Tenenbaum, William T. Freeman, and Antonio Torralba. GAN dissection: Visualizing and understanding generative adversarial networks. In *International Conference on Learning Representations (ICLR)*, 2019.

[34] Erik Häkkinen, Aaron Hertzmann, Jaakkko Lehtinen, and Sylvain Paris. GANSpace: Discovering interpretable GAN controls. *Advances in Neural Information Processing Systems*, 33:9841–9850, 2020.

[35] Been Kim, Martin Wattenberg, Justin Gilmer, Carrie Cai, James Wexler, Fernanda Viegas, and Rory Sayres. Interpretability beyond feature attribution: Quantitative testing with concept activation vectors (TCAV). In *Proceedings of the 35th International Conference on Machine Learning*, volume 80 of *Proceedings of Machine Learning Research*, pages 2668–2677, 2018.

[36] Ali Rahimi and Benjamin Recht. Random features for large-scale kernel machines. In *Advances in Neural Information Processing Systems*, volume 20, pages 1177–1184, 2007.

[37] Rajarshi Chitta, Rong Jin, Timothy C. Havens, and Anil K. Jain. Approximate kernel k-means: Solution to large scale kernel clustering. In *Proceedings of the 17th ACM SIGKDD International Conference on Knowledge Discovery and Data Mining*, pages 895–903, 2011.

[38] Ninh Dang Pham and Rasmus Pagh. Fast and scalable polynomial kernels via explicit feature maps. In *Proceedings of the 19th ACM SIGKDD International Conference on Knowledge Discovery and Data Mining*, pages 239–247, 2013.

[39] Matthew Tancik, Pratul P. Srinivasan, Ben Mildenhall, Sara Fridovich-Keil, Nithin Raghavan, Utkarsh Singhal, Ravi Ramamoorthi, Jonathan T. Barron, and Ren Ng. Fourier features let networks learn high frequency functions in low dimensional domains. In *Advances in Neural Information Processing Systems*, volume 33, pages 7537–7547, 2020.

[40] Danica J Sutherland and Jeff Schneider. On the error of random fourier features. *arXiv preprint arXiv:1506.02785*, 2015.

[41] Jonathan Ho and Tim Salimans. Classifier-free diffusion guidance. *arXiv preprint arXiv:2207.12598*, 2022.

[42] Dustin Podell, Zion English, Kyle Lacey, Andreas Blattmann, Tim Dockhorn, Jonas Müller, Joe Penna, and Robin Rombach. Sdxl: Improving latent diffusion models for high-resolution image synthesis, 2023.

[43] Junsong Chen, Chongjian Ge, Enze Xie, Yue Wu, Lewei Yao, Xiaozhe Ren, Zhongdao Wang, Ping Luo, Huchuan Lu, and Zhenguo Li. Pixart- σ : Weak-to-strong training of diffusion transformer for 4k text-to-image generation, 2024.

[44] Abhimanyu Dubey Aaron Grattafiori et al. The llama 3 herd of models, 2024.

[45] Gemma-Team. Gemma 3 technical report, 2025.

[46] DeepSeek-AI, Daya Guo, Dejian Yang, Haowei Zhang, Jun-Mei Song, et al. Deepseek-r1 incentivizes reasoning in llms through reinforcement learning. *Nature*, 645(8081):633–638, September 2025.

[47] Qwen-Team. Qwen3 technical report, 2025.

[48] Yann LeCun, Corinna Cortes, and C. J. C. Burges. Mnist handwritten digit database. *ATT Labs [Online]*, 2010.

[49] Yaroslav Ganin, Evgeniya Ustinova, Hana Ajakan, Pascal Germain, Hugo Larochelle, François Fleuret, Mario Marchand, and Victor Lempitsky. Domain-adversarial training of neural networks. *Journal of Machine Learning Research*, 2016.

[50] Tsung-Yi Lin, Michael Maire, Serge Belongie, Lubomir Bourdev, Ross Girshick, James Hays, Pietro Perona, Deva Ramanan, C. Lawrence Zitnick, and Piotr Dollár. Microsoft coco: Common objects in context, 2015.

[51] Tom Kwiatkowski, Jennimaria Palomaki, Olivia Redfield, Michael Collins, Ankur Parikh, Chris Alberti, Danielle Epstein, Illia Polosukhin, Matthew Kelcey, Jacob Devlin, Kenton Lee, Kristina Toutanova, Llion Jones, Ming-Wei Chang, Andrew Dai, Jakob Uszkoreit, Quoc Le, and Slav Petrov. Natural questions: a benchmark for question answering research. *Transactions of the Association for Computational Linguistics*, 2019.

[52] Nils Reimers and Iryna Gurevych. Sentence-bert: Sentence embeddings using siamese bert-networks. *Proceedings of the 2019 Conference on Empirical Methods in Natural Language Processing*, nov 2019.

[53] Danica J Sutherland, Heiko Strathmann, Michael Arbel, and Arthur Gretton. Efficient and principled score estimation with nyström kernel exponential families. In *International Conference on Artificial Intelligence and Statistics*, pages 652–660. PMLR, 2018.

Appendix A Proofs

A.1 Proof of Proposition 1

We start by writing the empirical covariance-difference operator explicitly. By definition,

$$\widehat{\Lambda}_{X,Y|T} = \frac{1}{n} \sum_{i=1}^n \phi_{\otimes}(t_i, x_i) \phi_{\otimes}(t_i, x_i)^\top - \frac{\eta}{m} \sum_{j=1}^m \phi_{\otimes}(t'_j, y_j) \phi_{\otimes}(t'_j, y_j)^\top.$$

Consider the following stacked feature matrices:

$$\Psi_X = \begin{bmatrix} \phi_{\otimes}(t_1, x_1)^\top \\ \vdots \\ \phi_{\otimes}(t_n, x_n)^\top \end{bmatrix} \in \mathbb{R}^{n \times D}, \quad \Psi_Y = \begin{bmatrix} \phi_{\otimes}(t'_1, y_1)^\top \\ \vdots \\ \phi_{\otimes}(t'_m, y_m)^\top \end{bmatrix} \in \mathbb{R}^{m \times D},$$

where $D = d_T d_X$. Then, we can write

$$\widehat{\Lambda}_{X,Y|T} = \Psi^\top \begin{bmatrix} \frac{1}{n} I_n & 0 \\ 0 & -\frac{\eta}{m} I_m \end{bmatrix} \Psi, \quad \Psi = \begin{bmatrix} \Psi_X \\ \Psi_Y \end{bmatrix}.$$

Next, consider the corresponding kernel matrix

$$K_{X,\eta Y|T} = \begin{bmatrix} \frac{1}{n} K_{TT} \odot K_{XX} & \frac{1}{\sqrt{nm}} K_{TT'} \odot K_{XY} \\ -\frac{\eta}{\sqrt{nm}} K_{TT'}^\top \odot K_{XY}^\top & -\frac{\eta}{m} K_{T'T'} \odot K_{YY} \end{bmatrix}.$$

Using the tensor-product identity $\langle \phi_T(t) \otimes \phi_X(x), \phi_T(t') \otimes \phi_X(x') \rangle = k_T(t, t') k_X(x, x')$, we observe that

$$K_{X,\eta Y|T} = \begin{bmatrix} \Psi_X \\ \Psi_Y \end{bmatrix} \begin{bmatrix} \frac{1}{n} I_n & 0 \\ 0 & -\frac{\eta}{m} I_m \end{bmatrix} \begin{bmatrix} \Psi_X \\ \Psi_Y \end{bmatrix}^\top = \Psi \begin{bmatrix} \frac{1}{n} I_n & 0 \\ 0 & -\frac{\eta}{m} I_m \end{bmatrix} \Psi^\top.$$

Hence, the following equations hold

$$\widehat{\Lambda}_{X,Y|T} = \Psi^\top D \Psi, \quad K_{X,\eta Y|T} = \Psi D \Psi^\top, \quad D = \text{diag}\left(\frac{1}{n} I_n, -\frac{\eta}{m} I_m\right).$$

It is a standard linear-algebra fact that the matrices $\Psi^\top D \Psi$ and $\Psi D \Psi^\top$ have the same nonzero eigenvalues (due to flipped multiplication order). Therefore, $\widehat{\Lambda}_{X,Y|T}$ and $K_{X,\eta Y|T}$ share the same nonzero spectrum. Finally, let $u = [u_{1:n}; u_{(n+1):(n+m)}]$ be an eigenvector of $K_{X,\eta Y|T}$ with eigenvalue $\lambda \neq 0$. Define vector v as follows:

$$v = \Psi^\top u = \sum_{i=1}^n u_i \phi_{\otimes}(t_i, x_i) + \sum_{j=1}^m u_{n+j} \phi_{\otimes}(t'_j, y_j).$$

Then, we have the following

$$\widehat{\Lambda}_{X,Y|T} v = \Psi^\top D \Psi \Psi^\top u = \Psi^\top D (K_{X,\eta Y|T} u) = \lambda \Psi^\top u = \lambda v,$$

which proves that v is an eigenvector of $\widehat{\Lambda}_{X,Y|T}$ associated with the same eigenvalue λ . This completes the proof.

A.2 Proof of Theorem 1

First, we show the unbiasedness and boundedness of the random-feature product kernel. By Bochner's theorem, for shift-invariant $k_T(t, t') = \kappa_T(t - t')$ and $k_X(x, x') = \kappa_X(x - x')$, there exist spectral measures μ_T, μ_X such that

$$k_T(t, t') = \mathbb{E}_{\omega_t \sim \mu_T} [\cos(\omega_t^\top (t - t'))], \quad k_X(x, x') = \mathbb{E}_{\omega_x \sim \mu_X} [\cos(\omega_x^\top (x - x'))].$$

Using independence between $\omega_{t,\ell}$ and $\omega_{x,\ell}$, and the identity $\cos(a)\cos(b) = \frac{1}{2}\cos(a+b) + \frac{1}{2}\cos(a-b)$, we may equivalently use the single cosine feature to represent the product kernel:

$$\begin{aligned}\mathbb{E}\left[g_\ell((t,x), (t',x'))\right] &= \mathbb{E}_{\omega_t, \omega_x}\left[\cos(\omega_t^\top(t-t') + \omega_x^\top(x-x'))\right] \\ &= \mathbb{E}_{\omega_t}\left[\cos(\omega_t^\top(t-t'))\right] \mathbb{E}_{\omega_x}\left[\cos(\omega_x^\top(x-x'))\right] \\ &= k_T(t, t') k_X(x, x').\end{aligned}\tag{6}$$

Moreover, for every ℓ and every pair of inputs,

$$|g_\ell((t,x), (t',x'))| \leq 1, \quad |\tilde{k}_\otimes((t,x), (t',x'))| \leq 1.\tag{7}$$

Next, we decompose the matrix as an average of i.i.d. bounded matrices. To do this, define $N := n + m$, and for every $\ell \in [r]$, consider the *single-feature* block matrix $K_{X,\eta Y|T}^{(\ell)} \in \mathbb{R}^{N \times N}$ by

$$K_{X,\eta Y|T}^{(\ell)} = \begin{bmatrix} \frac{1}{n}G_{XX}^{(\ell)} & \frac{1}{\sqrt{nm}}G_{XY}^{(\ell)} \\ -\frac{\eta}{\sqrt{nm}}(G_{XY}^{(\ell)})^\top & -\frac{\eta}{m}G_{YY}^{(\ell)} \end{bmatrix},\tag{8}$$

where the entries are

$$\begin{aligned}(G_{XX}^{(\ell)})_{ij} &:= g_\ell((t_i, x_i), (t_j, x_j)), \quad i, j \in [n], \\ (G_{YY}^{(\ell)})_{jj'} &:= g_\ell((t_j, y_j), (t_{j'}, y_{j'})), \quad j, j' \in [m], \\ (G_{XY}^{(\ell)})_{ij} &:= g_\ell((t_i, x_i), (t_j, y_j)), \quad i \in [n], j \in [m].\end{aligned}$$

By construction of \tilde{k}_\otimes , the proxy matrix is the average of these blocks:

$$\widetilde{K}_{rX,\eta Y|T} = \frac{1}{r} \sum_{\ell=1}^r K_{X,\eta Y|T}^{(\ell)}.\tag{9}$$

Taking expectation and using equation 6 entrywise shows that

$$\mathbb{E}\left[K_{X,\eta Y|T}^{(\ell)}\right] = K_{X,\eta Y|T}.\tag{10}$$

From equation 7, every entry of $G_{XX}^{(\ell)}, G_{YY}^{(\ell)}, G_{XY}^{(\ell)}$ has magnitude at most 1. Hence,

$$\left\|\frac{1}{n}G_{XX}^{(\ell)}\right\|_F^2 \leq \sum_{i=1}^n \sum_{j=1}^n \left(\frac{1}{n}\right)^2 = 1,\tag{11}$$

$$\left\|\frac{1}{\sqrt{nm}}G_{XY}^{(\ell)}\right\|_F^2 \leq \sum_{i=1}^n \sum_{j=1}^m \left(\frac{1}{\sqrt{nm}}\right)^2 = 1,\tag{12}$$

$$\left\|\frac{\eta}{m}G_{YY}^{(\ell)}\right\|_F^2 \leq \sum_{j=1}^m \sum_{j'=1}^m \left(\frac{\eta}{m}\right)^2 = \eta^2.\tag{13}$$

Using the matrix formulation, we obtain the following

$$\begin{aligned}\left\|K_{X,\eta Y|T}^{(\ell)}\right\|_F^2 &\leq \left\|\frac{1}{n}G_{XX}^{(\ell)}\right\|_F^2 + \left\|\frac{1}{\sqrt{nm}}G_{XY}^{(\ell)}\right\|_F^2 + \left\|\frac{\eta}{\sqrt{nm}}(G_{XY}^{(\ell)})^\top\right\|_F^2 + \left\|\frac{\eta}{m}G_{YY}^{(\ell)}\right\|_F^2 \\ &\leq 1 + 1 + \eta^2 + \eta^2 = 2(1 + \eta^2)\end{aligned}\tag{14}$$

Therefore,

$$\|K_{X,\eta Y|T}^{(\ell)}\|_F \leq \sqrt{2+2\eta^2} \quad (15)$$

The same argument applied to the expectation in equation 10 yields $\|K_{X,\eta Y|T}\|_F \leq \sqrt{2+2\eta^2}$, and thus, by the triangle inequality,

$$\left\|K_{X,\eta Y|T}^{(\ell)} - K_{X,\eta Y|T}\right\|_F \leq \|K_{X,\eta Y|T}^{(\ell)}\|_F + \|K_{X,\eta Y|T}\|_F \leq \sqrt{8+8\eta^2} \quad (16)$$

Now, we consider the Hilbert space $(\mathbb{R}^{N \times N}, \langle \cdot, \cdot \rangle_F)$. Consider the centered random matrices

$$X_\ell := K_{X,\eta Y|T}^{(\ell)} - K_{X,\eta Y|T}, \quad \ell = 1, \dots, r.$$

Then, X_1, \dots, X_r are i.i.d. random vectors satisfying $\mathbb{E}[X_\ell] = 0$, and by equation 16, $\|X_\ell\|_F \leq 4$ almost surely. A Hoeffding inequality for Hilbert-space-valued random vectors ([53, Lemma 11]) implies that, for every $\delta \in (0, 1)$, with probability at least $1 - \delta$,

$$\left\| \frac{1}{r} \sum_{\ell=1}^r X_\ell \right\|_F \leq \frac{4}{\sqrt{r}} \left(1 + \sqrt{2 \log \frac{1}{\delta}} \right). \quad (17)$$

Since $\frac{1}{r} \sum_{\ell=1}^r X_\ell = \widetilde{K}_{rX,\eta Y|T} - K_{X,\eta Y|T}$ by equation 9 and $\mathbb{E}[K^{(\ell)}] = K$, we obtain

$$\|\widetilde{K}_{rX,\eta Y|T} - K_{X,\eta Y|T}\|_F \leq \sqrt{\frac{8+8\eta^2}{r}} \left(1 + \sqrt{2 \log \frac{1}{\delta}} \right). \quad (18)$$

Since both $K_{X,\eta Y|T}$ and $\widetilde{K}_{rX,\eta Y|T}$ are symmetric, the Hoffman–Wielandt inequality gives

$$\|\boldsymbol{\lambda}(K_{X,\eta Y|T}) - \boldsymbol{\lambda}(\widetilde{K}_{rX,\eta Y|T})\|_2 \leq \|\widetilde{K}_{rX,\eta Y|T} - K_{X,\eta Y|T}\|_F. \quad (19)$$

Combining these two inequalities proves the stated inequality.

Applying PromptSplit on Stable Diffusion XL Prompts and Different Styles Generated Pictures

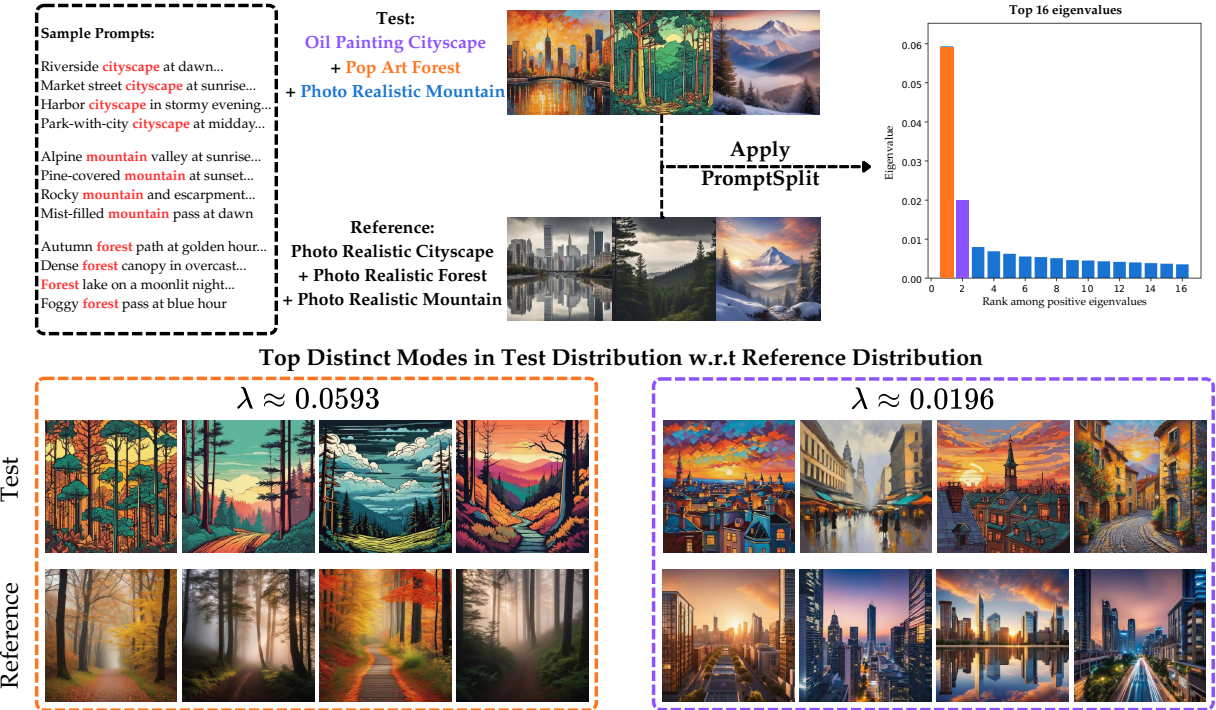


Figure 5: PromptSplit detected style and scene disagreements in a controlled text-to-image setting. (Top) Sample prompts, generated outputs, and bar plot of top 16 eigenvalues. (Bottom) Strongest samples for top identified distinct modes.

Appendix B Additional Numerical Results

B.1 Image Style Disagreement.

In figure 1 we generated three clusters of prompts and sampled 1000 images per cluster with different styles. For test dataset we used oil painting style for cityscape images, and pop art style for forests which differs from photo realistic style images generated for reference. We also generated photo realistic mountain images for both test and reference datasets. PromptSplit kernel-based algorithm successfully identified the two distinct modes in style with significant larger eigenvalues.

B.2 Answer Distribution Disagreement Detection

We compare Llama 3.2 (Test) and Gemma 3 (Reference) on three prompt clusters (Figure 6 for celebrity, American city, and fast modern fuel car, using 100 prompts per cluster and 10,000 generated answers per cluster (30,000 prompt–answer pairs per model)). The per-cluster answer dispersions show a clear difference in answer generation: Gemma collapses strongly onto one or two dominant entities in all clusters, while Llama’s answers are more distributed across multiple names. Applying PromptSplit to the aggregated prompt–answer pairs yields a small number of dominant test-dominant disagreement directions, and the leading samples for these modes isolate interpretable, cluster-specific differences (top three modes respectively shows entities in celebrities, modern cars, and cities that are most different from the reference set answers) which aligns with variations in prompt/answer behaviors visible in the dispersions.

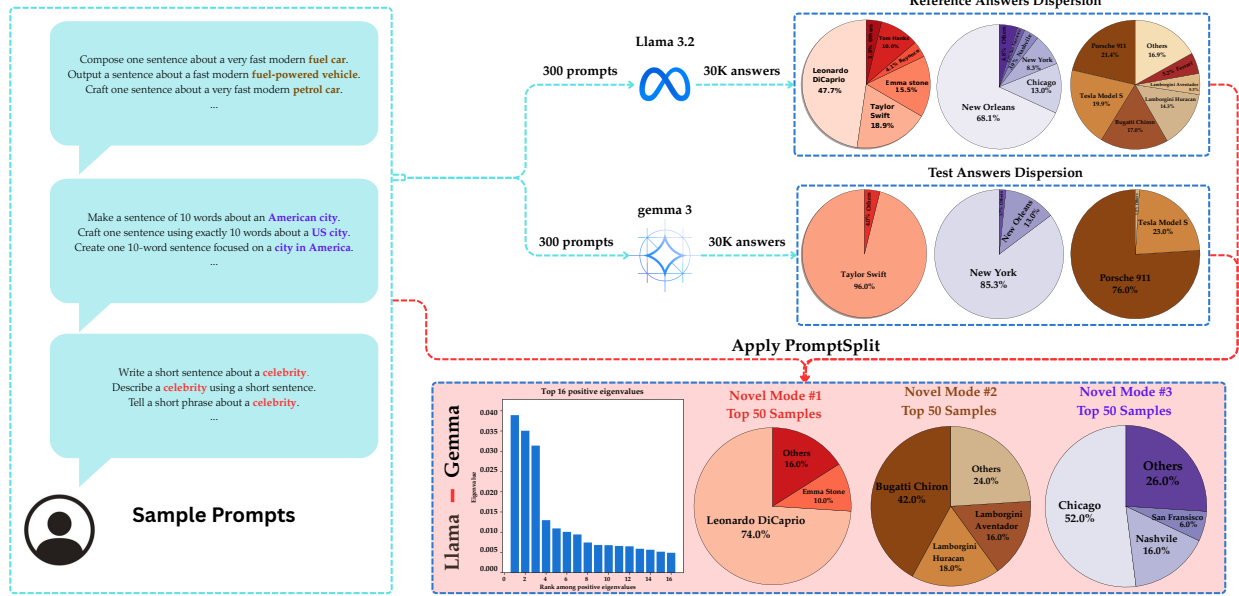


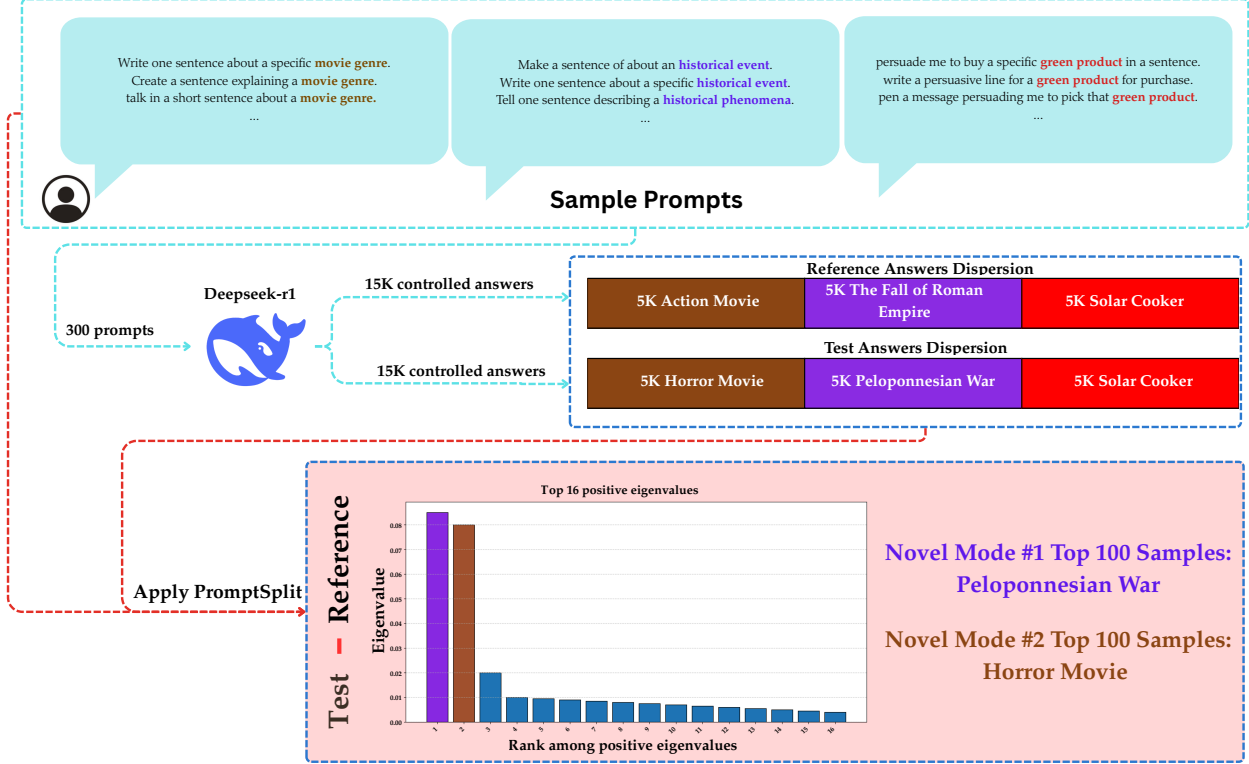
Figure 6: PromptSplit reveals prompt-dependent answer-mode differences between Llama 3.2 (test) and Gemma 3 (reference) on three prompt clusters (celebrity, American city, and fast modern fuel car). Top: per-cluster empirical answer dispersion for each model, highlighting differences in concentration vs. diversity. Bottom: PromptSplit identified three clusters with leading positive eigenvalues (left) and top answers only generated by test model.

B.3 Controlled Answers Disagreement.

To validate that PromptSplit can recover known differences, we construct a controlled text-to-text setting (Figure 7) where both “reference” and “test” outputs are produced by the same DeepSeek-r1 [46] model, but with different answer-control constraints. Prompts are partitioned into three clusters, and the control is intentionally applied so that the test condition differs from the reference primarily in the movie-genre and historical-phenomena clusters, while the third cluster is a control where reference and test are intended to match. We apply PromptSplit by embedding prompts and answers, constructing a joint prompt–answer similarity structure, and computing the leading eigen-directions of the covariance-difference operator, where large positive eigenvalues indicate the most prominent test-dominant disagreement modes. The resulting eigenspectrum shows two dominant positive modes, consistent with the two clusters where answers were deliberately shifted, and inspecting the leading samples for these modes demonstrates human-interpretable differences (Horror w.r.t Action and Poleponnesian War w.r.t The Fall of Roman Empire) that align with the intended controlled shifts.

B.4 Ablation Study on Number of random Fourier features

We evaluate projection dimension $r \in \{800, 1500, 2000, 3000, 5000\}$ on the full 30k-pair SDXL vs. PixArt- Σ comparison ($\eta = 1$, DINOv2-giant + Sentence-BERT embeddings, bandwidth selected via eigenvalue-gap heuristic) (Figures 8, 9). At $r = 800$, primary modes are recovered but eigenvalues are compressed and smaller modes noisier. By $r = 1500\text{--}2000$, eigenvalue magnitudes increase, mode ranking stabilizes, and prompt attribution sharpens. At $r = 3000$ (default), top modes match those at $r = 5000$ almost identically in spectrum shape, prompt semantics, and visual patterns. These results align with Theorem 1 $O(1/\sqrt{r})$ eigenvalue–vector bound and confirm that modest r suffices for approximation of leading disagreement directions at scale.



B.5 Ablation Study on Number of Samples

To investigate the effect of dataset size on the quality and stability of the detected disagreement modes, we evaluate the random-projection variant of PromptSplit across varying numbers of prompt–output pairs (Figures 10, 11). We use the MS-COCO 2014 validation set (30k captions) as the base and create subsampled versions with $n = m \in \{5k, 10k, 20k, 30k, 50k, 90k\}$ pairs per model/dataset. All experiments employ the same hyperparameters ($r = 3000$, $\eta = 1$, DINOv2-giant + Sentence-BERT embeddings, bandwidth selected via eigenvalue-gap heuristic). Figure X (top row) shows the top-10 eigenvalues and the strongest-attributed prompts/images for the pairwise comparison SDXL vs. PixArt- Σ across different sample sizes. We observe that:

- With as few as 5k–10k samples, the method already identifies the dominant disagreement modes (e.g., tennis-court geometry, plate placement, ramp/sideboard composition), with the largest eigenvalues corresponding to semantically consistent prompt clusters, however there are minor flaws in some modes.
- At 30k samples (the full MS-COCO val2014 size), eigenvalue magnitudes stabilize, and the ranking of top modes becomes highly consistent with the full-dataset run. Beyond 30k (up to 90k subsampled with replacement from the same caption pool), further gains are marginal: the top 3–5 modes remain nearly identical in attributed prompts and visual patterns, while smaller modes show minor fluctuations due to sampling variance.
- Beyond 30k (up to 90k generated with different seeds from the same 30K caption), further gains are

marginal: the top 3–5 modes remain nearly identical in attributed prompts and visual patterns, while smaller modes show minor fluctuations due to added samples disagreements.

These results indicate that PromptSplit is robust even at moderate sample sizes and 30k pairs are typically sufficient to reliably recover the principal directions of prompt-dependent disagreement in real-world text-to-image settings. Importantly, the kernel-based (non-projected) formulation becomes computationally prohibitive beyond 10K-15K samples ($O((n + m)^3)$ scaling), showing the necessity of the random-projection approximation for large-scale analysis. Runtime measurements (single A5000 GPU) are reported in Table 1.

B.6 Synthetic Gaussian Mixture.

In a controlled synthetic study (Figure 12), eight 50-dimensional Gaussian components simulate test embeddings and eight simulate reference embeddings, with 8-dimensional one-hot prompts shared within each cluster and 100 samples per component; joint projections visibly separate clusters and the eigen-spectrum of the covariance-difference operator behaves predictably: when the test and reference mixtures differ in k components, PromptSplit yields k positive and k negative principal eigenvalues, while when all components coincide, the spectrum collapses near zero—empirically validating that the method detects precisely the number and directionality of cluster-level disagreements.

B.7 Additional NQ-Open Experiments

Figures 13, 14, 15 extend the NQ-Open study to additional LLM pairs and show that PromptSplit isolates prompt-conditioned disagreement in a consistent, interpretable way across comparisons. In each figure, we report the leading positive eigenmodes and we qualitatively inspect the highest-attribution question clusters to reveal the prompt families that most strongly separate the two models’ behaviors. Across pairs, the dominant modes typically correspond to coherent topical categories (e.g., particular entity-centric question types), where the models diverge in answer selection, factual framing, or phrasing. Importantly, alongside these high-disagreement directions, we also include a representative low-eigenvalue (or “similar”) mode which shows questions that receive weak attribution under PromptSplit and yield largely aligned answers across the two models.

B.8 Disagreement Identification on MS-COCO Captions.

We generated images using three state-of-the-art text-to-image models—Stable Diffusion XL (SDXL), PixArt- Σ , and Kandinsky on the 30,000 captions from the MS-COCO 2014 validation set. Due to the large dataset size, we applied the scalable random-projection variant of PromptSplit (with projection dimension $r = 3000$) to identify prompt clusters that induce systematic behavioral disagreements in the generated images (Figures 16, 17, 18, 19, 20, 21)

We performed pairwise comparisons between each pair of models (SDXL vs. PixArt- Σ , SDXL vs. Kandinsky, PixArt- Σ vs. Kandinsky) as well as comparisons of each model against the real MS-COCO validation images (serving as a reference distribution). For each comparison, the top 5 identified modes of disagreement with the largest positive eigenvalues. Each mode is illustrated a selection of generated (or real reference) images.

These visualizations highlight interpretable prompt families where the models diverge in visual style, composition, object placement, realism, or alignment with the input text, complementing aggregate metrics such as FID or CLIPScore that do not capture prompt-conditioned differences.

<p>Distinct Mode #1 $\lambda = 4.94 \times 10^{-2}$</p> <p>1: A baseball player holding a bat on top of a field. 2: A baseball player holding a bat on a field. 3: The baseball pitcher has wound up his arm to pitch that ball. 4: A baseball player holding a baseball bat on a field.</p> <p></p> <p>Prompts Test: SDXL Reference: PixartΣ</p>	<p>Distinct Mode #2 $\lambda = 1.64 \times 10^{-3}$</p> <p>1: A woman with a cigarette standing, while a group of people with luggage walk towards a bus. 2: A man in a red shirt rides a yellow surfboard on light blue water. 3: A man rides a water slide surfboard into the ocean and splash from the shore. 4: A man holding a surf board in his hands walking towards the beach.</p> <p></p> <p>Prompts Test: SDXL Reference: PixartΣ</p>	<p>Distinct Mode #3 $\lambda = 1.36 \times 10^{-3}$</p> <p>1: A male tennis player in action on the court. 2: A man holding a tennis racket running to hit the ball. 3: A tennis player in action on the court. 4: A man swinging a tennis racket at a ball on a field.</p> <p></p> <p>Prompts Test: SDXL Reference: PixartΣ</p>	<p>Distinct Mode #4 $\lambda = 1.27 \times 10^{-3}$</p> <p>1: A man and a woman ride an elephant for the first time. 2: a group of people sitting at a table with plates of food 3: A truck and people on an elephant are travelling down the road. 4: Several plates of food are set on a table.</p> <p></p> <p>Prompts Test: SDXL Reference: PixartΣ</p>	<p>Distinct Mode #5 $\lambda = 9.58 \times 10^{-4}$</p> <p>1: some people are taking pictures of a pizza 2: Three dogs bite at a frisbee while at a park. 3: Drawing of a surfer riding a large wave. 4: A group of people are eating a pizza.</p> <p></p> <p>Prompts Test: SDXL Reference: PixartΣ</p>	<p>Distinct Mode #6 $\lambda = 7.70 \times 10^{-4}$</p> <p>1: A open metal oven with a rack for cooking. 2: a person talking a pic of pizza on the counter 3: The man is in his refrigerator looking for something to eat or drink 4: A nice cooking smart phon with a sticker on it</p> <p></p> <p>Prompts Test: SDXL Reference: PixartΣ</p>
<p>Distinct Mode #1 $\lambda = 5.07 \times 10^{-2}$</p> <p>1: A man walking down a beach holding a surf board. 2: A man holding a surf board in his hands walking towards the beach. 3: A man walking down a beach with a surfboard in hand. 4: A woman walking in ocean next to a white surfboard.</p> <p></p> <p>Prompts Test: SDXL Reference: PixartΣ</p>	<p>Distinct Mode #2 $\lambda = 1.33 \times 10^{-3}$</p> <p>1: A giraffe in a grassy field near a surfboard. 2: A group of giraffes in a grassy area by fences. 3: A giraffe standing in the grass near a tree. 4: A big zebra and a small zebra are standing in a grassy field.</p> <p></p> <p>Prompts Test: SDXL Reference: PixartΣ</p>	<p>Distinct Mode #3 $\lambda = 1.94 \times 10^{-3}$</p> <p>1: A young man doing a flip on a skateboard in the middle of a busy street. 2: a person on a surf board jumps in the air over snow. 3: A man skateboards on the rim of a skate pipe in front of a crowd. 4: A boy does a jump with a skateboard while a girl watches.</p> <p></p> <p>Prompts Test: SDXL Reference: PixartΣ</p>	<p>Distinct Mode #4 $\lambda = 1.01 \times 10^{-3}$</p> <p>1: A blue snowboard sitting on top of a snow covered slope. 2: A few people that are standing with skateboards. 3: A group of men riding skateboards up the side of a wooden ramp. 4: A snowboard sitting on a snow covered slope.</p> <p></p> <p>Prompts Test: SDXL Reference: PixartΣ</p>	<p>Distinct Mode #5 $\lambda = 9.01 \times 10^{-4}$</p> <p>1: a group of beginner snow skiers having class. 2: a person on skis with ski poles in snow. 3: A person riding a snowboard across a snow covered slope. 4: A skier in a squat position on skies skiing downhill.</p> <p></p> <p>Prompts Test: SDXL Reference: PixartΣ</p>	<p>Distinct Mode #6 $\lambda = 8.59 \times 10^{-4}$</p> <p>1: A man is taking a bite from a piece of pizza. 2: There is a pizza with some slices taken out of it. 3: A few pieces of pizza sitting on a plate. 4: a man smile at a table with a pizza on it.</p> <p></p> <p>Prompts Test: SDXL Reference: PixartΣ</p>
<p>Distinct Mode #1 $\lambda = 5.27 \times 10^{-2}$</p> <p>1: A person sitting on a wooden bench outside. 2: A picture of a person standing by a bicycle. 3: Two people sitting on a bench while a dog looks at them. 4: An adult stands near the counter in a kitchen.</p> <p></p> <p>Prompts Test: SDXL Reference: PixartΣ</p>	<p>Distinct Mode #2 $\lambda = 1.32 \times 10^{-3}$</p> <p>1: A young man riding a white surfboard on top of a wave. 2: A young man riding a wave on his surf board. 3: A man watersurfing on a white board in choppy water. 4: A man riding a wave on top of a surfboard.</p> <p></p> <p>Prompts Test: SDXL Reference: PixartΣ</p>	<p>Distinct Mode #3 $\lambda = 1.21 \times 10^{-3}$</p> <p>1: A giraffe standing next to a zebra on a field. 2: A giraffe in a grassy field near a hill. 3: A giraffe running across a grass covered field. 4: A giraffe and a zebra are in a grassy field.</p> <p></p> <p>Prompts Test: SDXL Reference: PixartΣ</p>	<p>Distinct Mode #4 $\lambda = 1.06 \times 10^{-3}$</p> <p>1: a tennis player holding a tennis racket on a court. 2: a woman swinging a tennis racquet on a tennis court. 3: a man on a tennis court swinging a racket towards a ball. 4: a man swinging a racquet on a tennis court.</p> <p></p> <p>Prompts Test: SDXL Reference: PixartΣ</p>	<p>Distinct Mode #5 $\lambda = 8.92 \times 10^{-4}$</p> <p>1: a pizza cut into slices on a plate. 2: a plate with cut slices of pizza and pepperoni. 3: A plate topped with a slice of pizza, a chicken breast and vegetables. 4: A knife and a pizza cut into slices on the plate.</p> <p></p> <p>Prompts Test: SDXL Reference: PixartΣ</p>	<p>Distinct Mode #6 $\lambda = 8.47 \times 10^{-4}$</p> <p>1: Guy jumping with his skateboard doing tricks on the sidewalk. 2: Man preforming stunt on skateboard outside in the city. 3: There are two men riding on a skateboard on the street. 4: two people riding skate boards on a city street</p> <p></p> <p>Prompts Test: SDXL Reference: PixartΣ</p>

Figure 8: Top six modes identified by PromptSplit comparing SDXL - PixartΣ generatead images on MS-COCO with different Random Fourier features (RFF) r ranging from 1000 to 2000

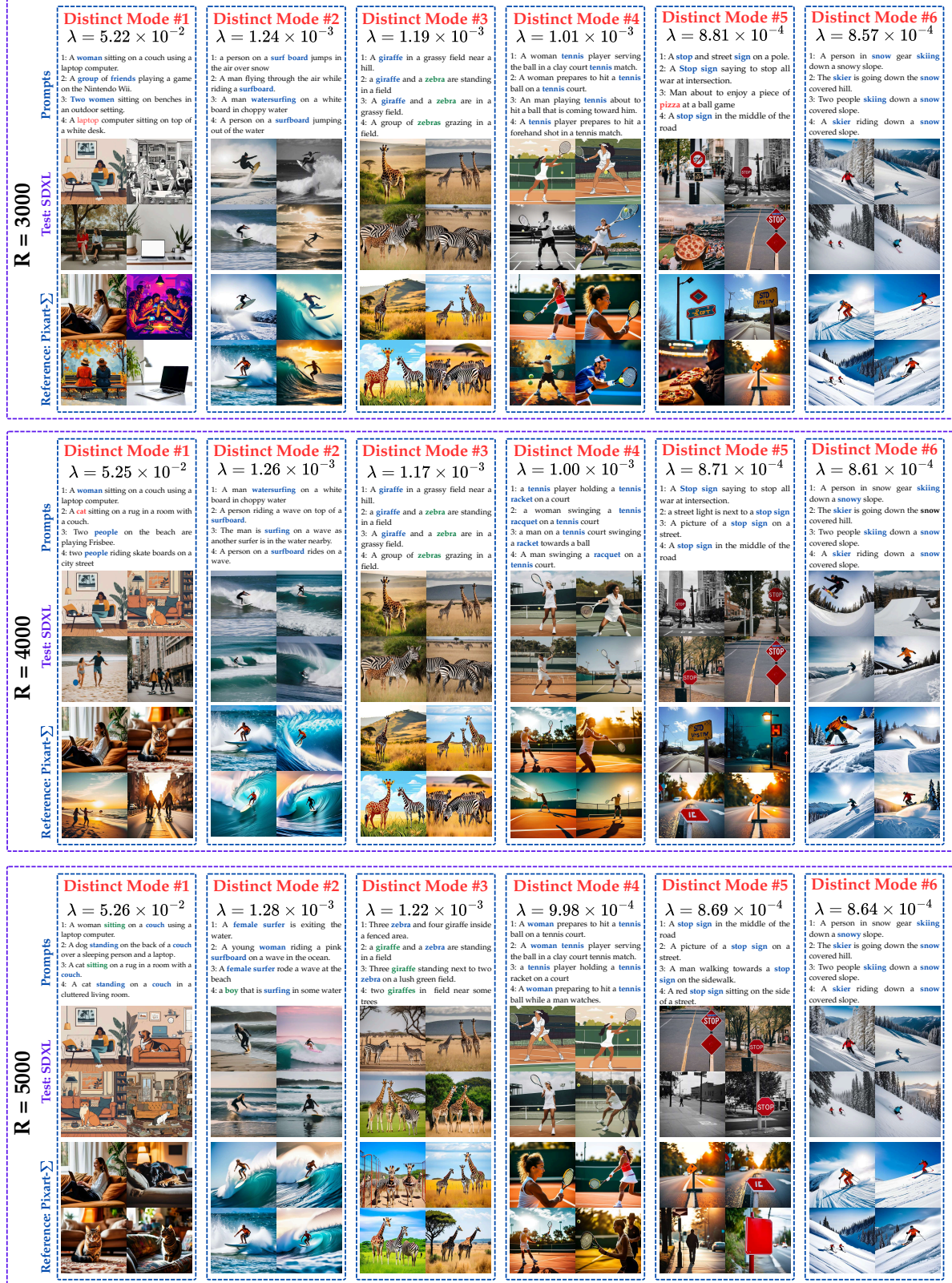


Figure 9: Top six modes identified by PromptSplit comparing SDXL - Pixart Σ generatead images on MS-COCO with different Random Fourier features (RFF) r ranging from 3000 to 6000

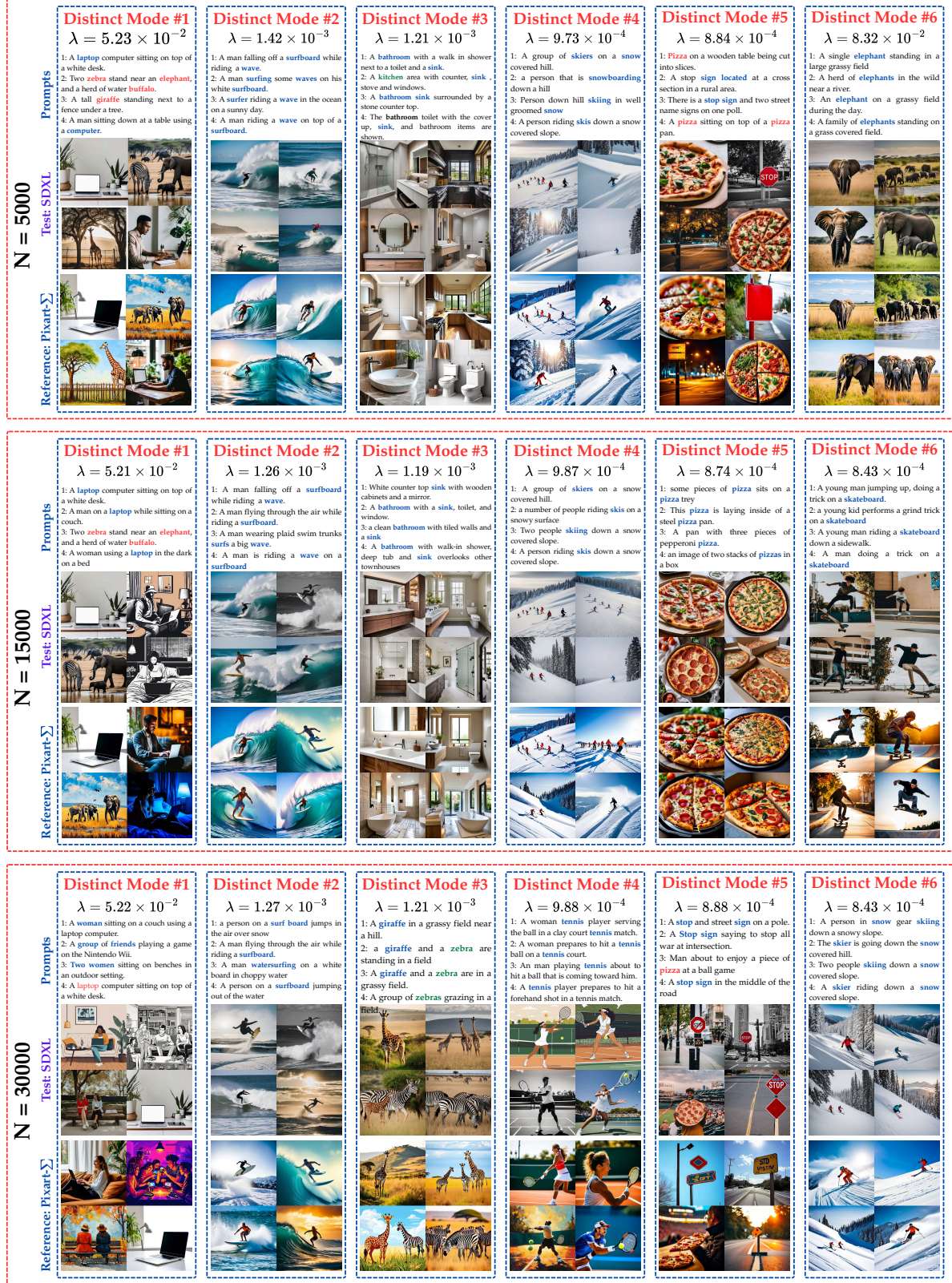


Figure 10: Top six modes identified by PromptSplit comparing SDXL - Pixart Σ generatead images on MS-COCO with different number of samples n ranging from 5000 to 30000



Figure 11: Top six modes identified by PromptSplit comparing SDXL - Pixart Σ generatead images on MS-COCO with different number of samples n ranging from 45000 to 90000

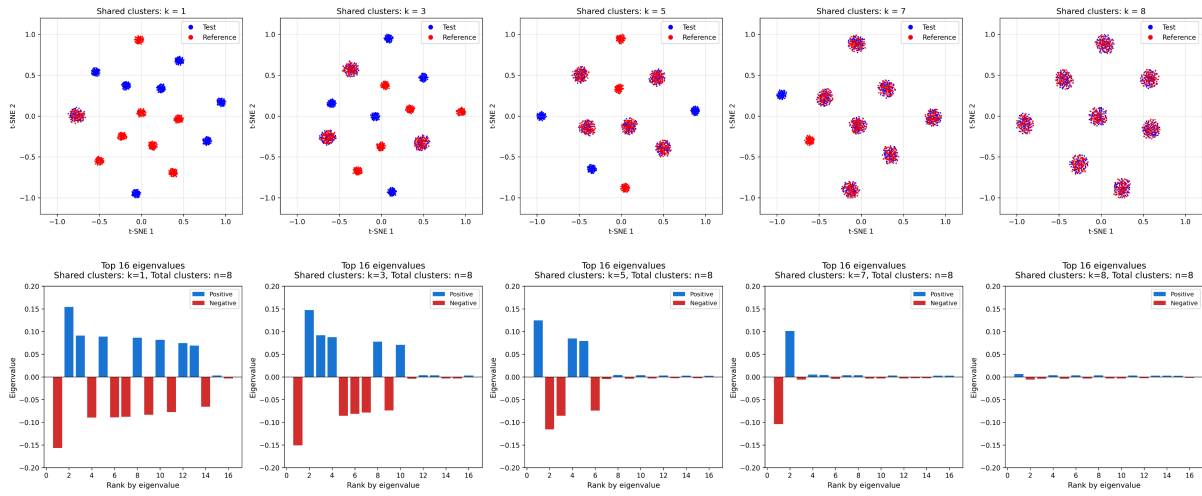


Figure 12: PromptSplit identified the numbers of distinct modes with significant large eigenvalues

Gemma 3 × NQ-Open — Llama 3.2 × NQ-Open		
Prompts (NQ-Open)	Test: Gemma 3	Reference: Llama 3.2
Distinct Mode #1 $\lambda = 1.12 \times 10^{-2}$ 1: singer in the movie let there be light 2: who played bane in the dark knight rises 3: who played jessica buchanan on one life to live 4: who sang phantom of the opera for the movie 5: who plays catwoman in the dark knight rises	Test: Gemma 3 1: Nina Petrova 2: Javier Bardem 3: Brianna Bertolotti. 4: Sarah Brightman 5: Shelley Conn.	Reference: Llama 3.2 1: Clint Eastwood. 2: Tom Hardy. 3: Kassie Mehlhoffer 4: Michael Crawford. 5: Anne Hathaway.
Distinct Mode #2 $\lambda = 3.79 \times 10^{-3}$ 1: who sang it just the way it is 2: who sang it's a long way to the top 3: who sang the song we've got tonight 4: who sang come and get your love now 5: who sang this is how we do it	Test: Gemma 3 1: U2 2: Chuck Berry 3: Rod Stewart. 4: The Black Eyed Peas 5: Björk	Reference: Llama 3.2 1: Willie Nelson. 2: AC/DC. 3: Elton John. 4: Redbone. 5: Montell Jordan.
Distinct Mode #3 $\lambda = 2.91 \times 10^{-3}$ 1: who scored the most goals in premier league 2: who scored the most goals in a premier league season 3: who won the most superbows in the nfl 4: which nfl team has the most super bowls 5: who has won the most championships in the nfl	Test: Gemma 3 1: Erling Haaland. 2: Ruud van Nistelrooy... 3: The New England Patriots (6) 4: New England Patriots (6) 5: The Dallas Cowboys...	Reference: Llama 3.2 1: Alan Shearer (260). 2: Alan Shearer... 3: The Pittsburgh Steelers... 4: The Pittsburgh Steelers... 5: The Pittsburgh Steelers with 17.
Similar Mode $\lambda = 6.85 \times 10^{-8}$ 1: which bird is the film happy feet about 2: who is the god of fire in norse mythology 3: hydrogen peroxide is the substrate for which enzyme 4: who plays arturo on the young and restless 5: when was the court of the lions built	Test: Gemma 3 1: Penguins! 2: Surtur 3: Catalase 4: Michael Bolton 5: Around 1185 AD.	Reference: Llama 3.2 1: The penguin. 2: Surtur. 3: Catalase. 4: I'm not sure... 5: The Court ... was built in 1185.

Figure 13: PromptSplit detected top distinct modes for 20000 generated short answers for test (Gemma3) w.r.t reference (Llama3.2) over NQ-Open questions as prompts.

Llama 3.2 × NQ-Open — NQ-Open × NQ-Open		
Prompts (NQ-Open)	Test: Llama 3.2	Reference: NQ-Open
Distinct Mode #1 $\lambda = 4.59 \times 10^{-3}$	1: when did the iphone 5 first come out 2: when was windows 7 service pack 1 released 3: when did samsung galaxy note 3 come out 4: when did ipad pro 2nd generation come out 5: when did the ipad pro second generation come out	1: September 2012. 2: August 2012. 3: August 2013. 4: October 2013. 5: October 2016.
Distinct Mode #2 $\lambda = 2.44 \times 10^{-3}$	1: who wrote you made me so very happy 2: who wrote the song i believe in you 3: who sang the song can't live if living is without you 4: who wrote the song i've been everywhere 5: who wrote send a message to my heart	1: I don't have a specific answer... 2: ... written by Stevie Wonder. 3: ... was sung by Sam Cooke. 4: Rolf Harris... 5: ... by Paul McCartney ...
Distinct Mode #3 $\lambda = 2.19 \times 10^{-3}$	1: who plays black widow in iron man 2 2: who played the robot girl in small wonder 3: who plays the grandmother in switched at birth 4: actress who played emily walters in the recent movie hampstead 5: who played anne frank in the original movie	1: Scarlett Johansson. 2: Molly Ringwald. 3: Lea Thompson. 4: Helen Mirren. 5: Helen Mirren.
Similar Mode $\lambda = 4.02 \times 10^{-4}$	1: who has the most career homeruns in mlb 2: who has hit the most home runs in major league baseball 3: who won ncaa womens basketball championship in 2017 4: who won the women's ncaa in 2017 5: when did england last reach a semi final world cup	1: Barry Bonds (762) 2: Barry Bonds (762) 3: South Carolina. 4: South Carolina. 5: 2018 World Cup.

Figure 14: PromptSplit detected top distinct modes for 20000 generated short answers for test (Llama 3.2) w.r.t reference (NQ-Open Answers) over NQ-Open questions as prompts.

NQ-Open × NQ-Open — Llama 3.2 × NQ-Open		
Prompts (NQ-Open)	Test: NQ-Open	Reference: Llama 3.2
Distinct Mode #1 $\lambda = 1.96 \times 10^{-2}$	1: when is a new episode of this is us coming out 2: when did the last episode of the originals air 3: when did season one of series of unfortunate events come out 4: when is the new show charmed coming out 5: when does season 5 episode 6 of the originals come out	1: September 26, 2017 2: June 23, 2017 3: January 13, 2017 4: October 14, 2018 5: May 30, 2018
Distinct Mode #2 $\lambda = 4.56 \times 10^{-3}$	1: what year did the us host the world cup of soccer 2: when is the last time brazil won world cup 3: when is the last time brazil won the world cup 4: when was the last world cup that brazil won 5: when did brazil win their last world cup	1: 1994 2: 2002 3: 2002 4: 2002 5: 2002
Distinct Mode #3 $\lambda = 2.91 \times 10^{-3}$	6384: when did the chicken pox vaccine come out in the us 16963: when was the chicken pox vaccine first given 19091: when was the first now that's what i call music 15590: when did the minimum drinking age become 21 14003: when did yuengling start brewing black and tan	1: ... in the US in 1995 by ... 2: First given in 1961. 3: ... in UK in 1983. 4: 1984, most ... in 1988. 5: ... since 1820.
Similar Mode $\lambda = 3.99 \times 10^{-4}$	1: who has sold the most albums all time 2: who has sold the most albums worldwide ever 3: who sold more records the beatles or michael jackson 4: who sold more records the beatles or rolling stones 5: who are the top 3 best selling music artists of all time	1: The Beatles 2: The Beatles 3: The Beatles 4: The Beatles 5: Elvis ... , The Beatles, ... Jackson

Figure 15: PromptSplit detected top distinct modes for 20000 short answers for test (NQ-Open) w.r.t generated answers for reference (Llama 3.2) over NQ-Open questions as prompts.

Reference Dataset:		Test Dataset:			
Pictures: PixArt generated with MS-COCO caption Prompts: MS-COCO captions		Pictures: SDXL generated with MS-COCO caption Prompts: MS-COCO captions			
Prompts	Novel Mode #1	Novel Mode #2	Novel Mode #3	Novel Mode #4	Novel Mode #5
PixArt (Test)	<p>1: A giraffe standing on top of a dirt field near trees. 2: A zebra standing on top of a lush green field. 3: A giraffe standing in dirt field next to trees. 4: A couple of zebra standing on top of a lush green field. 5: A couple of zebra standing on top of a lush green field. 6: A pair of zebra's leaning over eating grass in a field. 7: Three zebra standing on a road in a grassy field. 8: A herd of zebra standing on top of a dirt field. 9: A zebra eating grass next to a wire fence.</p>	<p>1: A young man riding a skateboard up the side of a ramp. 2: A man riding a skateboard on a wooden ramp. 3: A man riding a skateboard down a ramp. 4: A man riding a skateboard down the side of a ramp. 5: A man riding a skateboard up the side of a ramp. 6: A man riding a skateboard down a ramp. 7: A man riding a skateboard up the side of a ramp. 8: A young man riding a skateboard down a ramp. 9: A man riding a skateboard up the side of a ramp.</p>	<p>1: A baseball player holding a baseball bat on a field. 2: A baseball player swinging a bat on a field. 3: A baseball player holding a bat standing on a field. 4: A baseball player holding a bat on a baseball field. 5: A baseball player holding a bat on a field. 6: A baseball player holding a bat on a field. 7: A baseball player holding a bat while standing on a field. 8: A baseball player swinging a bat on a field. 9: A baseball player holding a bat on a field.</p>	<p>1: A white bus driving down a street near buildings. 2: A blue bus driving down a street past a park. 3: A red bus parked in front of a building. 4: A yellow and blue bus parked at the end of a street. 5: A baseball player holding a bat on a field. 6: A group of people standing on a beach flying a red kite. 7: A blue bus driving down a street next to trees. 8: A red bus traveling down a busy city street. 9: A pizza sitting on top of a white plate.</p>	<p>1: A cat laying on a cushion on top of a table. 2: A cat laying on top of a black office chair. 3: A cat sitting on a bed near a television remote. 4: A cat laying on a couch with a remote. 5: A cat laying on top of a blanket near a wall. 6: A cat is sleeping on the arm of a couch. 7: A cat laying on a bed by a window. 8: A cat laying on top of a bag sitting on a floor. 9: A cat laying on top of a couch.</p>
SDXL (Reference)					

Figure 16: PromptSplit detected top novel modes for 30000 pictures generated by test (Pixart- Σ) w.r.t reference model (SDXL) over MS-COCO captions as prompts.

Test Dataset:		Reference Dataset:				
Pictures: Kandinsky generated with MS-COCO caption		Pictures: MS-COCO Dataset Images				
Prompts: MS-COCO captions		Prompts: MS-COCO captions				
Prompts		Novel Mode #1	Novel Mode #2	Novel Mode #3	Novel Mode #4	Novel Mode #5
MS-COCO (Reference)	Kandinsky (Test)	<p>1: Zebras, an elephant and some giraffes stand together in the grass.</p> <p>2: A zebra is standing away from two adult giraffe.</p> <p>3: A zebra is standing on gravel, facing the camera,</p> <p>4: Two zebra standing next to each other on a dry grass field</p> <p>5: A zebra walking through the grass next to a bush.</p> <p>6: A big zebra and a small zebra are standing in a grassy field.</p> <p>7: A couple of zebra standing next to each other near a tree.</p> <p>8: A small herd of zebra standing next to each other.</p> <p>9: there are two zebras standing in the wild together</p>	<p>1: A woman standing in front of a mirror with bright blue hair.</p> <p>2: A woman using a smart phone with her two hands.</p> <p>3: Caucasian girl talking on a cell phone in public.</p> <p>4: A woman using a cell phone next to a laptop.</p> <p>5: A woman looking out the window of a train.</p> <p>6: A woman in vintage hat holding a tan suitcase.</p> <p>7: A woman is sitting using a cell phone.</p> <p>8: A young woman holds a cell phone to her ear.</p> <p>9: A beautiful woman standing on the side of a road next to a street.</p>	<p>1: a couple of elephants fighting in a grass area</p> <p>2: A small herd of elephants are standing around each other</p> <p>3: there are two elephants that are walking in the wild together</p> <p>4: A man standing near an elephant with its trunk outstretched.</p> <p>5: two huge elephant with tusks hidden among the trees</p> <p>6: An elephant is walking along with another elephant.</p> <p>7: Two elephants that are standing in the dirt.</p> <p>8: Two baby elephants are playing at the feet of two adult elephants.</p> <p>9: The elephant is standing on the grass in the clearing.</p>	<p>1: A cat on a toilet seat of some sort.</p> <p>2: A cat looks at the camera while sitting on the laptop.</p> <p>3: A cat is looking at the camera while lying down on the chair</p> <p>4: A cat that is laying on top of a bed.</p> <p>5: A cat laying on top of a wooden shelf with boxes.</p> <p>6: a cat stares into the camera while sitting on a blanket</p> <p>7: A long haired cat laying on a shoe on the floor.</p> <p>8: A cat laying on top of a cat bed.</p> <p>9: there is a cat that is drinking out of the toilet</p>	<p>1: A man standing on top of a sandy beach near a colorful kite.</p> <p>2: People on a beach with a kite flying in the air.</p> <p>3: A man walking on the beach flying a kite.</p> <p>4: A woman standing on top of a sandy beach under a flying kite.</p> <p>5: A person that is flying a kite in the air.</p> <p>6: A man standing on a beach flying a kite.</p> <p>7: A child is shown holding a kite in the air.</p> <p>8: A man flying a kite above in a blue sky.</p> <p>9: People flying kites in the sand on a windy beach.</p>

Figure 17: PromptSplit detected top novel modes for 30000 pictures generated by test (Kandinsky) w.r.t reference (MS-COCO images) over MS-COCO captions as prompts.

Test Dataset:		Reference Dataset:				
Pictures: SDXL generated with MS-COCO caption		Pictures: MS-COCO Dataset Images				
Prompts: MS-COCO captions		Prompts: MS-COCO captions				
Novel Mode #1	Novel Mode #2	Novel Mode #3	Novel Mode #4	Novel Mode #5		
<p>1: A city street with cars and a bus on it. 2: Two giraffes are standing outside of a door. 3: A bus and truck driving down a busy city street. 4: A bus driving in a city area with traffic signs. 5: A double level bus on a street driving through a construction area. 6: Two giraffes are looking at each other in a wooden room. 7: A red fire hydrant on the side of a street. 8: A cat laying on a couch with a remote. 9: A cat sitting on the dashboard of a car.</p>	<p>1: A young man riding a skateboard up the side of a ramp. 2: A man riding a skateboard on a wooden ramp. 3: A man riding a skateboard down a ramp. 4: A man riding a skateboard down the side of a ramp. 5: A man riding a skateboard up the side of a ramp. 6: A man riding a skateboard down a ramp. 7: A man riding a skateboard up the side of a ramp. 8: A young man riding a skateboard down a ramp. 9: A man riding a skateboard up the side of a ramp.</p>	<p>1: A white toilet sitting next to a window in a bathroom. 2: A walk in shower next to a white sink. 3: A white toilet sitting in a bathroom under a white cabinet. 4: A shower and a white toilet in a small bathroom. 5: A white toilet sitting in a bathroom next to a sink. 6: A white toilet sitting in a bathroom next to a tile wall. 7: A bathroom with a white toilet sitting under a window. 8: A white toilet in a bathroom next to a white sink. 9: A white toilet sitting in a bathroom next to a white wall.</p>	<p>1: A pizza sitting on top of a white plate. 2: A slice of pizza sitting on top of a white plate. 3: A pizza sitting on top of a black plate. 4: A slice of pizza sitting on top of a white plate. 5: A piece of pizza sitting on top of a white plate. 6: A hand holding a piece of pizza with more pizza on a plate. 7: A large cheesy pizza sitting on top of a white plate. 8: A pizza sitting on top of a wooden cutting board. 9: A pizza sitting on top of a wooden cutting board.</p>	<p>1: A man standing on a tennis court holding a tennis racquet. 2: A man holding a tennis racquet on a tennis court. 3: A man swinging a tennis racquet on a tennis court. 4: A man holding a tennis racquet on a tennis court. 5: A man standing on a tennis court holding a racquet. 6: A man holding a tennis racquet on a tennis court. 7: A man standing on a tennis court with a tennis racquet. 8: A man standing on a tennis court holding a tennis racquet. 9: A man standing on a tennis court holding a tennis racquet.</p>		
SDXL (Test)						
MS-COCO (Reference)						

Figure 18: PromptSplit detected top novel modes for 30000 pictures generated by test (SDXL) w.r.t reference (MS-COCO images) over MS-COCO captions as prompts.

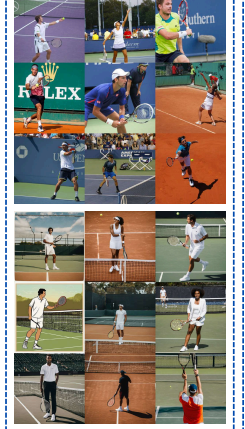
Test Dataset: Pictures: MS-COCO images Prompts: MS-COCO captions		Reference Dataset: Pictures: SDXL generated with MS-COCO caption Prompts: MS-COCO captions		
<p>Novel Mode #1</p> <p>1: A herd of giraffe standing around a lush green tree. 2: A couple of zebra standing on top of a lush green field. 3: A pair of zebra's leaning over eating grass in a field. 4: A giraffe standing on top of a dirt field near trees. 5: A group of giraffe walking across a dirt field. 6: A herd of zebra standing on top of a dirt field. 7: A herd of zebra standing on a lush green field. 8: A group of zebra standing on top of a lush green field. 9: A couple of zebra standing on top of a grass covered field.</p> 	<p>Novel Mode #2</p> <p>1: A man holding a tennis racquet on a tennis court. 2: A woman standing on a tennis court holding a tennis racquet. 3: A man holding a tennis racquet on a tennis court. 4: A man standing on a tennis court holding a tennis racquet. 5: A man standing on a tennis court holding a racquet. 6: A woman holding a tennis racquet on a tennis court. 7: A man standing on a tennis court holding a racquet. 8: A man holding a tennis racquet on a tennis court. 9: A man holding a tennis racquet on a tennis court.</p> 	<p>Novel Mode #3</p> <p>1: A young man riding a skateboard up the side of a ramp. 2: A man riding a skateboard up the side of a ramp. 3: A young man riding a skateboard down a ramp. 4: A man riding a skateboard up the side of a ramp. 5: A boy doing a trick on a skateboard off a ramp. 6: A man riding a skateboard up the side of a ramp. 7: A man riding a skateboard on top of a skate park. 8: A man doing a trick on a skate board. 9: A man riding a skateboard down the side of a ramp.</p> 	<p>Novel Mode #4</p> <p>1: A plate topped with a cheesy pizza on a table. 2: A pizza sitting on top of a white plate on a table. 3: A cheesy pizza sitting on top of a white plate. 4: A pizza sitting in a pizza box topped with pepperoni. 5: A large pizza sitting on a pizza pan with a slice missing. 6: A pizza sitting on top of a white plate covered in cheese and sauce. 7: A slice of pizza sitting on top of a white plate. 8: A pizza sitting on top of a wooden table. 9: A half eaten slice of pizza is on a plate with a knife and fork.</p> 	<p>Novel Mode #5</p> <p>1: A baseball player standing at home base with a bat. 2: A baseball player holding a bat standing on a field. 3: A baseball player holding a bat next to a base. 4: A baseball player swinging a bat near home base. 5: A baseball player with a bat on the field. 6: A baseball player holding a bat standing near home plate. 7: A baseball player swinging a bat over home plate. 8: A baseball player holding a bat over home plate. 9: A baseball player tossing a bat next to home plate.</p> 
SDXL (Reference) MS-COCO – SDXL Prompts				

Figure 19: PromptSplit detected top novel modes for 30000 images for test (MS-COCO) w.r.t reference (SDXL generated) over MS-COCO captions as prompts.

Test Dataset:		Reference Dataset:			
Pictures: Pixart- Σ generated with MS-COCO caption		Pictures: MS-COCO images			
Prompts: MS-COCO captions		Prompts: MS-COCO captions			
Prompts	Novel Mode #1	Novel Mode #2	Novel Mode #3		
MS-COCO (reference) Pixart- Σ — MS-COCO	<p>1: A man riding a surfboard on a wave in the ocean. 2: A man on a surfboard jumping over a wave. 3: A man riding a surfboard on a wave in the ocean. 4: A man riding a surfboard on a small wave in the ocean. 5: A man riding a surfboard on top of a wave. 6: A man riding a white surfboard on a wave in the ocean. 7: A man riding a surfboard on top of a wave. 8: A man floating on top of waves in the ocean holding a surfboard. 9: A man riding a surfboard on top of a wave.</p> 	<p>1: A man standing on a tennis court with a tennis racquet. 2: A man holding a tennis racquet on a tennis court. 3: A woman standing on a tennis court holding a tennis racquet. 4: A man standing on a tennis court holding a tennis racquet. 5: A man swinging a racquet on a tennis court. 6: A man holding a tennis racquet on a tennis court. 7: A man standing on a tennis court holding a tennis racquet. 8: A woman standing on a tennis court hitting a tennis ball. 9: A man holding a tennis racquet on a tennis court.</p> 	<p>1: A man doing a trick on a skateboard on a ramp. 2: A man who is performing a trick on a skateboard. 3: A man who is performing a trick on a skateboard. 4: A man does a jump on a skateboard. 5: A young man riding a skateboard up the side of a ramp. 6: A man on a skateboard who is performing a trick. 7: A man performing a trick on a ledge on a skateboard. 8: A man riding a skateboard on a wooden ramp. 9: A man riding a skateboard down the side of a ramp.</p> 	<p>1: A couple of giraffe standing on top of a grass covered field. 2: A group of giraffe standing and sitting on a field. 3: A group of giraffe standing on top of a lush green field. 4: A giraffe standing in dirt field next to trees. 5: A giraffe standing next to a zebra on a field. 6: A giraffe standing on top of a dirt field near trees. 7: A group of giraffe walking across a dirt field. 8: Two giraffes that are standing together in a field. 9: A herd of giraffe standing on top of a grass covered field.</p> 	<p>1: A man riding skis down a snow covered slope. 2: A man riding skis down a snow covered slope. 3: A man riding skis down a snow covered slope. 4: A man riding skis down a snow covered slope. 5: A woman riding skis down a snow covered slope. 6: A person riding skis down a snow covered slope. 7: A man riding skis down a snow covered slope. 8: A man riding skis down a snow covered slope. 9: A man riding skis down a snow covered slope.</p> 

Figure 20: PromptSplit detected top novel modes for 30000 pictures generated by test (Pixart- Σ) w.r.t reference (MS-COCO images) over MS-COCO captions as prompts.

Test Dataset:		Reference Dataset:	
Pictures: MS-COCO Dataset Images		Pictures: PixArt generated with MS-COCO caption	
Prompts: MS-COCO captions		Prompts: MS-COCO captions	
Novel Mode #1	Novel Mode #2	Novel Mode #3	Novel Mode #4
<p>1: A woman standing on a tennis court holding a tennis racquet. 2: A man standing on a tennis court holding a racquet. 3: A man holding a tennis racquet on a tennis court. 4: A man standing on a tennis court holding a tennis racquet. 5: A man standing on a tennis court with a tennis racquet. 6: A man holding a tennis racquet on top of a tennis court. 7: A man standing on a tennis court holding a racquet. 8: A man holding a tennis racquet on a tennis court. 9: A man standing on a tennis court holding a tennis racquet.</p>	<p>1: A man riding skis down a snow covered slope. 2: A woman riding skis down a snow covered slope. 3: A man riding skis down a snow covered slope. 4: A man riding skis down a snow covered slope. 5: A man riding skis down a snow covered slope. 6: A man riding skis down a snow covered slope. 7: A man riding skis down a snow covered slope. 8: A man riding skis on top of a snow covered slope. 9: A person riding skis down the side of a snow covered slope.</p>	<p>1: A yellow and blue fire hydrant sitting on a sidewalk. 2: Red and white fire hydrant sitting on the side of a city street. 3: A blue fire hydrant posed on a street corner in a city. 4: A calico cat sits on a cushion on a bench. 5: A man standing under a large clock tower next to the ocean. 6: A white toilet sitting in a bathroom next to a sink. 7: A large yellow school bus stopping on a road. 8: A cat is sitting under a purple umbrella. 9: A silver and red fire hydrant sitting next to a street.</p>	<p>1: A plate topped with a cheesy pizza on a table. 2: A pizza sitting on top of a white plate on a table. 3: A cheesy pizza sitting on top of a white plate. 4: A pizza sitting in a pizza box topped with pepperoni. 5: A large pizza sitting on a pizza pan with a slice missing. 6: A pizza sitting on top of a white plate covered in cheese and sauce. 7: A slice of pizza sitting on top of a white plate. 8: A pizza sitting on top of a wooden table. 9: A half eaten slice of pizza is on a plate with a knife and fork.</p>
Prompts			
MS-COCO (Test)			
PixArt (Reference)			

Figure 21: PromptSplit detected top novel modes for 30000 images for test (MS-COCO) w.r.t reference (Pixart- Σ generated) over MS-COCO captions as prompts.